EUROPEAN ORGANIZATION FOR NUCLEAR RESEARCH (CERN)

CERN-EP-2024-275
2026/01/15

CMS-EXO-22-013

Search for t-channel scalar and vector leptoquark exchange in the high-mass dimuon and dielectron spectra in proton-proton collisions at $\sqrt{s} = 13\,\text{TeV}$

The CMS Collaboration*

arXiv:2503.20023v3 [hep-ex] 13 Jan 2026

Abstract

A search for t-channel exchange of leptoquarks (LQs) is performed in dimuon and dielectron spectra using proton-proton collision data collected at $\sqrt{s} = 13\,\text{TeV}$ with the CMS detector at the CERN LHC. The data correspond to an integrated luminosity of $138\,\text{fb}^{-1}$. Eight scenarios are considered, in which up or down quarks couple to muons or electrons via a scalar or vector LQ exchange, for dilepton invariant masses above 500 GeV. The LQ masses are probed up to 5 TeV, beyond a regime probed by previous pair-production and single-production searches. The differential distributions of dilepton events are fit to templates that model the nonresonant LQ exchange and various standard model background processes. Limits are set on LQ-fermion coupling strengths for scalar and vector LQ masses in the 1–5 TeV range at 95% confidence level, establishing stringent limits on first- and second-generation LQs.

Published in the Journal of High Energy Physics as doi:10.1007/JHEP12(2025)052.

© 2026 CERN for the benefit of the CMS Collaboration. CC-BY-4.0 license

*See Appendix A for the list of collaboration members

1 Introduction

Leptoquarks (LQs) are hypothetical particles proposed to explain the similarities between the quark and lepton sectors of the standard model (SM). Leptoquarks were initially introduced in early extensions of the SM, for example, in grand unified theories based on the $SU(5)$ and $SO(10)$ groups [1–6], such as the Pati–Salam model [1], composite models [7, 8], and technicolor models [9–11]. Leptoquarks have also been proposed as mediators of interactions between SM and dark matter particles [12, 13], and appear in R-parity violating supersymmetry models [14]. Results from the Muon $g-2$ experiment in 2021 showed deviations in the experimental value of the anomalous magnetic moment of the muon to 0.46 ppm [15]. The deviation is reduced when updated lattice quantum chromodynamics (QCD) calculations are considered [16]. Although the tension of the $g-2$ measurements has been largely resolved by using these calculations, a massive LQ could contribute to the anomalous magnetic moment by mixing with the SM Higgs field [17], and thus move the theory even closer to the latest experimental result [18].

Leptoquarks are electrically charged, color-triplet bosons, either scalar or vector, that carry a baryon number (B), as well as a lepton number (L). They have a fermion number $F = 3B + L$ of 0 or -2; however, LQs with $F = -2$ can mediate proton decay, and stringent limits from dedicated proton decay searches have strongly constrained such LQs [19]. Distinctions between different LQs are based on their SM gauge group transformation properties, giving rise to twelve LQ multiplets. Only six families do not mediate proton decay. Leptoquarks are labeled as first-, second-, third-, or mixed-generation based on the SM quarks and leptons with which they interact.

The quark-LQ-lepton interaction is characterized by the LQ-fermion coupling constants y_{LQ} (g_{LQ}) for the scalar (vector) case. At colliders, LQs can be produced singly or in pairs, or manifest via t-channel exchange. The pair-production channel is dominated by gluon-gluon fusion, with a cross section proportional to the square of the strong coupling constant (α_{S}^2). Since this production mode proceeds via the strong interaction, it is insensitive to the LQ-fermion coupling, and results in the most stringent bounds at low LQ masses ($m_{\mathrm{LQ}} \sim 1\,\mathrm{TeV}$). The single-production cross section scales as $\alpha_{\mathrm{S}} y_{\mathrm{LQ}}^2$ ($\alpha_{\mathrm{S}} g_{\mathrm{LQ}}^2$), but the channel can be more sensitive than pair production at higher m_{LQ} or y_{LQ} (g_{LQ}). Finally, the t-channel exchange process, shown in Fig. 1, has a cross section proportional to y_{LQ}^4 (g_{LQ}^4), with additional contributions proportional to y_{LQ}^2 (g_{LQ}^2) from the interference with dilepton production via the Drell–Yan (DY) process. This channel can have superior sensitivity at even higher m_{LQ}, as its cross section decreases more slowly than for the other two channels, as a function of m_{LQ}.

Several searches for LQs have been performed by the ATLAS and CMS Collaborations. Third-generation scalar and vector LQs coupled to a tau (τ) lepton and a bottom (b) quark were studied in Refs. [20, 21], which considered single and pair production, as well as t-channel LQ exchange. The t-channel exchange process is the most sensitive channel at large m_{LQ} and y_{LQ} (g_{LQ}), excluding at 95% confidence level (CL) third-generation scalar (vector) LQs with masses of 0.5–1.5 (0.5–2.3) TeV for y_{LQ} (g_{LQ}) values larger than 1.8–3.5 (0.9–3.5). Searches for vector LQs in the $\tau\tau$ channel were reported in Ref. [22], in which m_{LQ} of 1–5 TeV were excluded for $g_{\mathrm{LQ}} > 0.8$–3.7 at 95% CL for a U_1 LQ in the Pati–Salam model.

For pair-produced scalar LQs coupled to first- and second-generation fermions, the most stringent limits have been set by ATLAS, excluding LQs with masses below 1.8 and 1.7 TeV at 95% CL, respectively, independent of y_{LQ} and assuming a branching fraction of 100% into a quark and a lepton [23]. Single production of first- and second-generation scalar LQs has been studied by CMS [24], in which m_{LQ} below 1.73 TeV and 530 GeV, respectively, were excluded, assuming

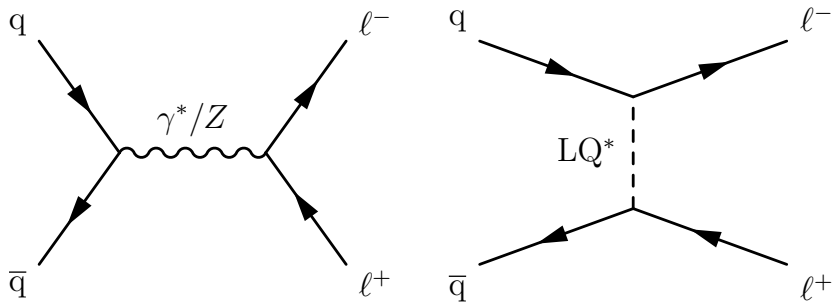


Figure 1: Leading order Feynman diagrams for SM DY production (left) and t-channel LQ exchange (right). The LQ amplitude interferes with the Z/γ^* amplitude.

$g_{LQ} = 1$ and a branching fraction of 100% into a quark and a lepton. Pair production of first- and second-generation scalar LQs have also been studied by CMS [25, 26]. First-generation scalar m_{LQ} were excluded up to 1.44 TeV at 95% CL, and second-generation scalar m_{LQ} were excluded up to 1.53 TeV, independent of y_{LQ} and assuming a branching fraction of 100% into a quark and a lepton. The CMS Collaboration has also studied pair production of first- and second-generation vector LQs, leading to exclusions of m_{LQ} up to 1.5 (1.3) TeV assuming Yang–Mills (minimal) couplings, and m_{LQ} less than 1.7 (1.1) TeV assuming minimal-minimal (absolute minimal) couplings, for a branching fraction of 100% into a quark and a lepton [27].

Motivated by the phenomenological studies performed in Refs. [28, 29], three families of LQs are considered: two scalar doublet families, R_2 and $\widetilde{R}_2$, and one vector triplet family, U_3. The subscripts refer to the dimensionality of the $SU(2)$ representation. Within the R_2, $\widetilde{R}_2$, and U_3 families, first- and mixed-generation LQs that couple up and down quarks to electrons and muons are considered. For the scalar doublet families, following Ref. [28], the case where the LQ couples only to right-handed quark multiplets and left-handed lepton multiplets (RL) is considered. The LQs are assumed to couple to a single quark and lepton, resulting in four scalar LQ coupling scenarios: two R_2 LQs, S_{eu} and $S_{\mu u}$, and two $\widetilde{R}_2$ LQs, S_{ed} and $S_{\mu d}$, where the subscripts denote the SM fermions. Similarly, four U_3 vector LQs are considered: V_{eu}, $V_{\mu u}$, V_{ed}, and $V_{\mu d}$. The SM gauge group transformation properties for the chosen LQ models are summarized in Table 1. The R_2 LQs appear in potential solutions to the muon anomalous magnetic moment problem [30, 31], $\widetilde{R}_2$ LQs appear in beyond-the-SM extensions for lepton flavor universality violation involving sterile neutrinos [31, 32], and U_3 LQs appear in models that describe scenarios for lepton flavor violation [33].

Table 1: Properties of the R_2, $\widetilde{R}_2$, and U_3 LQs from Ref. [19]. This paper describes a search for R_2 LQs with RL couplings and charge 5/3, $\widetilde{R}_2$ LQs with RL couplings and charge 2/3, and U_3 LQs with charges 2/3 and 5/3.

LQ family	$(SU(3), SU(2), U(1))$	Spin	Charge
R_2	(3, 2, 7/6)	0	5/3, 2/3
$\widetilde{R}_2$	(3, 2, 1/6)	0	2/3, -1/3
U_3	(3, 3, 2/3)	1	5/3, 2/3, -1/3

The LQ-quark-lepton interactions are defined by the following terms in the Lagrangian:

$$\mathcal{L} \supset y_{\ell u}\overline{u}_R\ell_L R^{5/3} + y_{\ell d}\overline{d}_R\ell_L\widetilde{R}^{2/3} + g_{\ell u}\overline{u}_L\gamma^\mu\ell_L U_\mu^{5/3} + g_{\ell d}\overline{d}_L\gamma^\mu\ell_L U_\mu^{2/3} + \text{h.c.}, \quad (1)$$

where $y_{\ell u}$ ($y_{\ell d}$) are the couplings of the charge 5/3 (2/3) R_2 ($\widetilde{R}_2$) scalar LQs to fermions and $g_{\ell u}$ ($g_{\ell d}$) are the couplings of the charge 5/3 (2/3) vector U_3 LQs to fermions. The terms describing

couplings of LQs to neutrinos are omitted. A complete description of the LQ interactions, as well as a more detailed review of LQ physics in precision experiments, can be found in Ref. [19].

This paper describes the first search for the t-channel exchange of LQs coupled to first- and second-generation SM fermions, probing scalar and vector LQs with masses in the range 1–5 TeV. The search uses proton-proton (pp) collision data at $\sqrt{s} = 13$ TeV corresponding to an integrated luminosity of 138 fb^{-1}, collected by the CMS experiment at the CERN LHC in 2016–2018. The hypothetical signal process results in the nonresonant exchange of muon or electron pairs. It is distinguished from the dominant background of SM DY events using the differential distributions of the dilepton invariant mass, the angle between the incoming quark and the outgoing lepton, and the rapidity of the dilepton system. The observed dilepton distributions are fit with a combination of signal and background templates, both produced by reweighting simulated SM DY events.

The paper is divided into ten sections. The analysis strategy is discussed in Section 2, followed by a description of the CMS detector and event reconstruction in Section 3. The simulated samples used for the signal and background estimation are described in Section 4, and the criteria used to select dimuon and dielectron events are described in Section 5. Section 6 contains a detailed discussion of the various backgrounds for this search, and how they are estimated. The procedure to build templates of the signal and background distributions is described in Section 7, followed by a discussion of the various systematic uncertainties that affect the measurements in Section 8. The results of maximum likelihood fits to data are discussed in Section 9, along with the limits at 95% CL on eight LQ couplings as functions of m_{LQ}. Finally, the paper is summarized in Section 10.

Tabulated results are provided in the HEPData record for this analysis [34].

2 Analysis strategy

The t-channel LQ exchange occurs in conjunction with the SM DY process, which is the primary background for this search. This analysis utilizes three variables computed from the dilepton system: the invariant mass, $m_{\ell\ell}$; the rapidity y; and $\cos\theta^*$ (abbreviated as c_*), the cosine of the angle between the quark (as opposed to the antiquark) and the lepton (as opposed to the antilepton) in the Collins–Soper frame (dilepton rest frame) [35, 36]. At a pp collider, the direction of the incident quark is unknown. Instead, an approximation is used, defined as $\cos\theta_{\text{R}} \equiv \frac{p_z}{|p_z|} c_*$, abbreviated as c_{R}, where p_z stands for the longitudinal momentum of the dilepton system. This approximation uses the fact that the quark will typically have higher longitudinal momentum than the antiquark, and hence, the longitudinal momentum of the dilepton system will more often align with that of the quark. The observed distributions in these three variables can be expressed as a convolution of the underlying differential cross section:

$$f(m^{\text{r}}_{\ell\ell},\, y^{\text{r}},\, c_{\text{R}}) = C \int \mathrm{d}m_{\ell\ell}\, \mathrm{d}y\, \mathrm{d}c_* R(m^{\text{r}}_{\ell\ell},\, y^{\text{r}},\, c_{\text{R}};\, m_{\ell\ell},\, y,\, c_*)\varepsilon(m_{\ell\ell},\, y,\, c_*)\frac{\mathrm{d}^3\sigma}{\mathrm{d}m_{\ell\ell}\, \mathrm{d}y\, \mathrm{d}c_*}, \quad (2)$$

where the superscript r distinguishes reconstructed variables from generator-level variables, C is a normalization constant, R is a resolution function that incorporates detector resolution and parton shower effects, and ε is an efficiency function. Since the convolution is a linear function of the cross section, σ, the resulting reconstructed distribution can be expressed as a sum of convolutions of different contributions to the total cross section. The linearity allows the expected observation for a given signal hypothesis to be represented as a sum of templates that are individually independent of the parameters of interest. Specifically, the parton-level

differential cross section of the SM DY process can be written as:

$$\left[\frac{\mathrm{d}\sigma}{\mathrm{d}c_*}(m_{\ell\ell}^2)\right]_{\mathrm{DY}} \propto \frac{3}{8}\left\{(1+c_*^2) + A_4 c_* + \frac{A_0}{2}\left(1-3c_*^2\right)\right\}, \tag{3}$$

where A_4 and A_0 are the standard dimensionless coefficients parametrizing the angular distribution of the DY process [37, 38]. The first two terms correspond to the leading order (LO), and the third term corresponds to next-to-LO (NLO). The coefficients A_0 and A_4 are functions of $m_{\ell\ell}$, the transverse momentum (p_{T}), and y of the dilepton system. Measurements of A_0 probe higher-order corrections in perturbative QCD, whereas A_4 is directly related to the SM forward-backward asymmetry, $A_{\mathrm{FB}} = (\sigma_{\mathrm{F}} - \sigma_{\mathrm{B}})/(\sigma_{\mathrm{F}} + \sigma_{\mathrm{B}}) = \frac{3}{8}A_4$, where σ_{F} and σ_{B} are the cross sections for forward ($c_* > 0$) and backward ($c_* < 0$) events, respectively. A measurement of A_{FB} and A_0 was recently performed by CMS [36].

The LO double-differential cross section for DY production that includes the t-channel exchange of a scalar LQ can be expressed as [28]:

$$\begin{aligned}\frac{\mathrm{d}^2\sigma}{\mathrm{d}m_{\ell\ell}\mathrm{d}c_*} \propto \left[\frac{\mathrm{d}^2\sigma}{\mathrm{d}m_{\ell\ell}\mathrm{d}c_*}\right]_{\mathrm{DY}} &+ y_{\mathrm{LQ}}^4 N_{\mathrm{pure}}^S(m_{\ell\ell})\left(\frac{1-c_*}{1-c_*+\frac{2m_{\mathrm{LQ}}^2}{m_{\ell\ell}^2}}\right)^2 \\ &+ y_{\mathrm{LQ}}^2 N_{\mathrm{int}}^S(m_{\ell\ell})\left[\frac{(1-c_*)^2}{1-c_*+\frac{2m_{\mathrm{LQ}}^2}{m_{\ell\ell}^2}}\right],\end{aligned} \tag{4}$$

and the differential cross section for a vector LQ exchange can be expressed as:

$$\begin{aligned}\frac{\mathrm{d}^2\sigma}{\mathrm{d}m_{\ell\ell}\mathrm{d}c_*} \propto \left[\frac{\mathrm{d}^2\sigma}{\mathrm{d}m_{\ell\ell}\mathrm{d}c_*}\right]_{\mathrm{DY}} &+ g_{\mathrm{LQ}}^4 N_{\mathrm{pure}}^V(m_{\ell\ell})\left(\frac{1+c_*}{1-c_*+\frac{2m_{\mathrm{LQ}}^2}{m_{\ell\ell}^2}}\right)^2 \\ &+ g_{\mathrm{LQ}}^2 N_{\mathrm{int}}^V(m_{\ell\ell})\left[\frac{(1+c_*)^2}{1-c_*+\frac{2m_{\mathrm{LQ}}^2}{m_{\ell\ell}^2}}\right],\end{aligned} \tag{5}$$

where $N_{\mathrm{pure}}^{S,V}$ and $N_{\mathrm{int}}^{S,V}$ are prefactors that depend on $m_{\ell\ell}$, and the vector and axial-vector couplings of the quark and lepton that couple to the LQ. The first LQ-specific term corresponds to pure t-channel LQ exchange, while the second term corresponds to the interference of the t-channel LQ exchange with the SM Z/γ^* diagram.

Following an approach similar to that of Ref. [36], the templates are histograms binned in three variables ($m_{\ell\ell}$, c_{R}, and y), constructed from simulated SM DY events that are reweighted using functions of the generator-level variables to represent each of the terms in Eqs. (4) or (5). A maximum likelihood fit of a linear combination of the templates to the observed data is performed to extract the signal and background parameters, namely A_0, A_4, and either y_{LQ} or g_{LQ}. The template construction is described in more detail in Section 7. Each of the eight combinations of spin and coupling to SM fermions is probed separately.

3 The CMS detector and event reconstruction

The central feature of the CMS apparatus is a superconducting solenoid of 6 m internal diameter, providing a magnetic field of 3.8 T. Within the solenoid volume are a silicon pixel and strip tracker, a lead tungstate crystal electromagnetic calorimeter (ECAL), and a brass and scintillator hadron calorimeter (HCAL), each composed of a barrel and two endcap sections. Forward calorimeters extend the pseudorapidity (η) coverage provided by the barrel and endcap detectors. Muons are detected in gas-ionization chambers embedded in the steel flux-return yoke outside the solenoid. A more detailed description of the CMS detector, together with a definition of the coordinate system used and the relevant kinematic variables, is reported in Ref. [39, 40].

Events of interest are selected using a two-tiered trigger system. The first level, composed of custom hardware processors, uses information from the calorimeters and muon detectors to select events at a rate of around 100 kHz within a fixed latency of about 4 μs [41]. The second level, known as the high-level trigger, consists of a farm of processors running a version of the full event reconstruction software optimized for fast processing, and reduces the event rate to around 1 kHz before data storage [42].

A particle-flow algorithm [43] aims to reconstruct and identify each individual particle in an event, with an optimized combination of information from the various elements of the CMS detector. The energy of photons is obtained from the ECAL measurement. The energy of electrons is determined from a combination of the electron momentum at the primary interaction vertex as determined by the tracker, the energy of the corresponding ECAL cluster, and the energy sum of all bremsstrahlung photons spatially compatible with originating from the electron track. The energy of muons is obtained from the curvature of the corresponding track. The energy of charged hadrons is determined from a combination of their momentum measured in the tracker and the matching ECAL and HCAL energy deposits, corrected for the response function of the calorimeters to hadronic showers. Finally, the energy of neutral hadrons is obtained from the corresponding corrected ECAL and HCAL energies. The primary vertex is taken to be the vertex corresponding to the hardest scattering in the event, evaluated using tracking information alone, as described in Section 9.4.1 of Ref. [44].

Muons are measured in the range $|\eta| < 2.4$, with detection planes made using three technologies: drift tubes, cathode strip chambers, and resistive-plate chambers. The single-muon trigger efficiency exceeds 90% over the full η range, and the efficiency to reconstruct and identify muons is greater than 96%. Matching muons to tracks measured in the silicon tracker results in a relative p_{T} resolution of 1% in the barrel and 3% in the endcaps for muons with $p_{\mathrm{T}} < 100\,\mathrm{GeV}$, and of better than 7% for muons in the barrel with $p_{\mathrm{T}} < 1\,\mathrm{TeV}$ [45].

The single-electron trigger efficiency is approximately 80% over the full η range, and the efficiency to reconstruct and identify electrons is greater than 65% for electrons with $p_{\mathrm{T}} > 20\,\mathrm{GeV}$. The momentum resolution for electrons with $p_{\mathrm{T}} \approx 45\,\mathrm{GeV}$ from $\mathrm{Z} \to \mathrm{ee}$ decays ranges from 1.7–4.5%. It is generally better in the barrel region than in the endcaps, and also depends on the bremsstrahlung energy emitted by the electron as it traverses the material in front of the ECAL [46].

Additional pp interactions within the same or nearby bunch crossings (pileup) can contribute additional tracks and calorimetric energy depositions, increasing the apparent jet momentum. To mitigate this effect, tracks identified as originating from pileup vertices are discarded and an offset correction is applied to correct for remaining contributions [47].

4 Simulated event samples

Various Monte Carlo (MC) event generators are used to simulate the SM background processes. The DY samples are generated at NLO in QCD with up to two extra partons using MADGRAPH5_aMC@NLO [48] v2.2.2 (v2.6.0) for samples corresponding to the 2016 (2017–2018) data-taking periods. The parton shower, hadronization, and quantum electrodynamics final-state radiation are simulated with PYTHIA v8.226 (v8.230) [49], using the FXFX merging scheme and the underlying event tune CUETP8M1 (CP5) [50, 51]. The NNPDF 3.0 parton distribution functions (PDFs) [52, 53] at NLO accuracy are used for samples corresponding to 2016, and NNPDF 3.1 [54] at next-to-NLO (NNLO) are used for 2017–2018. For consistency, all samples were reweighted to NNPDF 3.0 at NLO.

Additional backgrounds include diboson production (WW, WZ, ZZ), photon-induced dilepton production ($\gamma\gamma \to \ell\ell$), top quark pair production ($\mathrm{t\bar{t}}$), and single top quark production in association with a W boson (tW). The $\mathrm{t\bar{t}}$ and tW backgrounds are generated at NLO using POWHEG v2.0 [55–58], and interfaced with PYTHIA v8.226 (v8.230), with the CUETP8M2T4 (CP5) underlying event tune [59] for the 2016 (2017–2018) data-taking period. The diboson background samples are generated at NLO, with $\mathrm{ZZ} \to \ell\ell\ell'\ell'$, $\mathrm{ZZ} \to \ell\ell\nu\nu$, and $\mathrm{WW} \to \ell\nu\ell\nu$ processes generated using POWHEG [60, 61] and $\mathrm{WZ} \to \mathrm{qq}\ell\ell$, $\mathrm{WZ} \to \ell\ell\ell\nu$, and $\mathrm{ZZ} \to \mathrm{qq}\ell\ell$ processes generated using MADGRAPH5_aMC@NLO. All diboson samples are showered using PYTHIA and tune CUETP8M1 (CP5) for the 2016 (2017–2018) data-taking periods. The $\mathrm{t\bar{t}}$, tW, and diboson backgrounds use the NNPDF 3.0 (3.1) PDFs for 2016 (2017–2018) data-taking periods. The photon-induced background, $\gamma\gamma \to \ell\ell$, is simulated using the CEPGEN [62] implementation of LPAIR [63, 64], interfaced with PYTHIA v6.429 [65], using the Suri–Yennie proton structure function parametrization [66]. This contribution is split into three parts because the interaction at each proton vertex can be either elastic or inelastic.

The cross sections for the WZ and ZZ samples are normalized to the NLO predictions calculated with MCFM 6.6 [67], while the cross sections of the WW samples are normalized to the next-to-next-to-leading-logarithmic accuracy predictions [68]. The total cross section for the $\mathrm{t\bar{t}}$ process is normalized to the prediction with NNLO accuracy in QCD and next-to-next-to-leading-logarithmic accuracy for the soft-gluon radiation resummation calculated with TOP++ 2.0 [69].

Leptoquark signal samples modeled in the SLQRULES package [70] are generated using MADGRAPH5_aMC@NLO. These samples are used only for cross checks on the LQ template method.

The detector response for all MC samples is simulated using GEANT4 [71]. The pileup distribution in simulation is weighted to match the one observed in data.

5 Event selection

Events are required to have two leptons of same flavor and opposite charges. The dimuon and dielectron events are selected by single-muon and single-electron triggers, respectively. Dilepton triggers were not used as they had negligible gains over using single-lepton triggers. The events selected by the triggers are reconstructed and required to satisfy a number of offline requirements. The leading muon and electron p_{T} requirement is at least 40 GeV. The subleading lepton is required to have $p_{\mathrm{T}} > 15\,\mathrm{GeV}$. All muons are required to be within the acceptance of the muon system ($|\eta| < 2.4$), and all electrons must be within $|\eta| < 2.5$, excluding the barrel-endcap transition region of the ECAL ($1.44 < |\eta| < 1.57$) because the reconstruction of an electron object in this region is not optimal. Additionally, to remove cosmic ray muon induced

events, the azimuthal angle (ϕ) between the two muons is required to differ from π by more than 5 mrad.

Each reconstructed muon is required to pass identification criteria that are based on the number of hits observed in the tracker, the response of the muon detectors, and a set of matching criteria between muon track parameters, as measured by the inner tracker and muon detectors. To suppress nonprompt muons coming from heavy-flavor decays, each muon must be isolated from other particles in a cone of size $\Delta R = 0.4$ where $\Delta R = \sqrt{(\Delta\eta)^2 + (\Delta\phi)^2}$ refers to the distance from the muon to a given track. Further, the sum of the energy deposits of the charged and neutral hadrons divided by the muon track p_{T} within this cone should be less than 0.15. More details on the muon identification and reconstruction used in this analysis can be found in Refs. [45, 72].

The reconstructed electron candidates are required to pass identification criteria that are based on electromagnetic shower shape variables. Electrons originating from photon conversions are suppressed by requiring that the candidates have at most one missing inner tracker hit and not be consistent with being part of a conversion pair. Electrons are also required to be isolated from other particles within a cone of $\Delta R = 0.3$. The electron isolation criteria are based on the ratios of the electron p_{T} to the sum of energy deposits associated with the photons or hadrons. More details on the electron reconstruction and identification criteria used in this analysis are described in Ref. [46].

Events in the signal region (SR) must have $m_{\ell\ell} > 500$ GeV. This requirement suppresses $\mathrm{t\bar{t}}$ and nonprompt backgrounds. Additionally, the requirement has negligible impact on the signal sensitivity for heavy LQs ($m_{\mathrm{LQ}} > 1$ TeV), which primarily comes from events with $m_{\ell\ell} > 1$ TeV.

6 Backgrounds

The dominant background comes from DY events, and the subdominant background consists of fully leptonic decays of $\mathrm{t\bar{t}}$ events. Backgrounds from tW events, diboson processes, and leptonic decays of $\tau\tau$ originating from the DY process are also included. All of these backgrounds are modeled in simulation with a few corrections based on control samples in data. The estimated event yields of the $\mathrm{t\bar{t}}$, tW, $\tau\tau$, and diboson events are validated in data in a control region (CR) of $\mathrm{e}\mu$ events. A small fraction of the background comes from t-channel photon-induced dilepton production, which is modeled with MC simulation as well. Additionally, events where one or more jets are incorrectly identified as leptons also contribute to the total background yield. Such events are referred to as "MisID" events, primarily arising from W+jets processes and events composed uniquely of jets produced through the strong interaction, referred to as QCD multijet events. A technique based on CRs in data is employed to estimate the MisID contribution. For the dimuon (dielectron) channel, the total background from simulation and CR-based estimation consists of approximately 85 (82)% DY, 10 (9)% $\mathrm{t\bar{t}}$ plus tW, 5 (4)% diboson, and 0.5 (5)% MisID events.

The MisID background is estimated from data using the "misidentification rate" method [73, 74]. The misidentification rate is defined as the probability of a jet, having been reconstructed as a lepton candidate, to pass the lepton selection requirements outlined in Section 5. This rate is measured in a sample with two reconstructed leptons from a Z boson decay and an additional, potentially misidentified lepton. The two leptons corresponding to a Z boson decay are required to pass the lepton identification requirements and have an invariant mass within 7 GeV of the Z boson mass [75]. The third lepton candidate is used as a probe to measure the misidentification rate. This third lepton candidate is required to pass a less stringent set

of identification and isolation requirements than the full selection requirements of the analysis. The MisID background can then be estimated from CRs of data events with two lepton candidates: one region in which one lepton fails the full selection requirements, to model the W+jets events, and another region in which both leptons fail the requirements, to model the QCD multijet events. Events from these regions are assigned weights based on the expected misidentification probabilities of the failing lepton candidates. Contamination of this region by lepton pairs from DY and other prompt processes is subtracted using MC simulation. These reweighted events are used to estimate the yield and shape of the MisID background.

The MisID background estimation is validated in a CR with the same selection criteria as the SR, except the lepton pairs are required to have same-sign (SS) rather than opposite-sign (OS) charges. A large fraction of the events in this CR stem from misidentified jets. In the ee channel, there is a significant contribution to this sample from OS DY events where the charge of one of the electrons has been incorrectly assigned. The rate of charge misassignment in simulation is corrected using a sample of dilepton events near the Z peak with $70 < m_{\ell\ell} < 110\,\text{GeV}$. The MisID background estimate as well as MC estimates of other backgrounds are compared with the observed yield of SS events. A c_{R}-dependent correction to the MisID background estimate is calculated using the ratio of the MisID estimate to the number of observed SS events minus other backgrounds. The uncertainty in this correction is calculated as the quadratic sum of the statistical uncertainties from the limited sample size, the uncertainty in the number of DY pairs reconstructed as SS pairs, as well as a systematic uncertainty reflecting possible differences in shape between SS and OS MisID estimates.

The $\tau\tau$, tW, $\mathrm{t\bar{t}}$, and diboson backgrounds are validated in data using eμ events. The eμ CR has the same selection criteria as the SR, except that events are required to have one muon and one electron rather than pairs of same flavor. The CR is constructed from events that have a leading muon and a subleading electron, because samples with high-quality muons have lower contamination from misidentified leptons. The muon is required to have $p_{\text{T}} > 40\,\text{GeV}$ and pass the single-muon trigger, and the electron is required to have $p_{\text{T}} > 15\,\text{GeV}$. The identification and isolation criteria for muons and electrons are the same as in the SR. The MisID background is also present in this eμ CR and is estimated using the misidentification rate technique previously described. Good agreement is observed between the simulated and observed yields of eμ events across the entire mass range.

Because diboson events are produced via electroweak processes, they are expected to have a small forward-backward asymmetry in their lepton pairs; $\mathrm{t\bar{t}}$ events are also known to have an asymmetry, but it is too small to be detected using leptons alone [76]. The QCD and W+jets backgrounds are expected to have no asymmetry. Based on MC and CR estimates, an overall $A_{\text{FB}} \approx 0.01$ is predicted in the region of eμ events. The observed value in the eμ CR is $A_{\text{FB}} = 0.012 \pm 0.003$, consistent with this expectation.

Although the overall normalizations and asymmetries in eμ events are observed to be consistent between data and simulation, there are discrepancies between the predicted and observed shapes of the c_{R} distributions. To address these discrepancies, a correction is derived from the ratio of the c_{R} distributions in data and simulation in eμ events, and applied to the shape of the c_{R} distributions in simulation. Because the asymmetry is modeled well, this correction is derived symmetrically in c_{R} using four bins of $|c_{\text{R}}|$. A single correction is derived in the 500–3000 GeV mass range because of the limited event count. This correction modifies by 5–25% the shapes of the templates used to model the corresponding backgrounds in the SR. The statistical uncertainty in each of the four $|c_{\text{R}}|$ bins is modeled as a separate shape nuisance parameter.

Figure 2 shows a comparison between measured $\mu\mu$ and ee events and the background predic-

tion in the SR after all corrections have been applied. Good agreement is observed between the simulated and observed numbers of $\mu\mu$ and ee events.

7 Template construction

To model the dilepton differential distributions, parameter-independent templates are constructed for each piece of the differential cross section of LQ production shown in Eqs. (4) and (5). For the SM DY component, the differential cross section is reparametrized as follows:

$$\left[\frac{\mathrm{d}\sigma}{\mathrm{d}c_*}(m_{\ell\ell}^2)\right]_{\mathrm{DY}} \propto \frac{3}{4(2+\alpha)}\left\{(1+c_*^2)+\frac{(2+\alpha)}{2}\,A_4\,c_*+\alpha(1-c_*^2)\right\}, \tag{6}$$

where $\alpha = \frac{2A_0}{2-A_0}$. The first two terms are symmetric and antisymmetric in c_*, respectively, and the third term is proportional to α. The LQ exchange comprises two terms with coefficients y_{LQ}^4 or g_{LQ}^4 for the pure exchange of the LQ and, y_{LQ}^2 or g_{LQ}^2 for the interference with Z/γ^*. The templates for these five pieces of the cross section are denoted as f_{s} (symmetric), f_{a} (antisymmetric), and f_α (corresponding to the third term) for the three DY templates and $f_{\mathrm{LQ(pure)}}$ and $f_{\mathrm{LQ(int)}}$ for the pure and interference LQ terms, respectively.

In Ref. [36], the f_{s} , f_{a} , and f_α templates are constructed by binning events in c_{R} and reconstructed $|y|$. These templates are constructed for various mass regions, and the fit is performed for each mass region separately. In this paper, the two-dimensional templates are extended to three dimensions by additionally binning in the reconstructed $m_{\ell\ell}$. The templates are constructed by reweighting simulated DY events as analytical functions of generator-level quantities to match the differential distributions of the three pieces of the DY cross section. To reduce statistical fluctuations in the simulator, each event is used twice, once with $+c_*$ and once with $-c_*$, with a weight of 0.5 to keep the normalization unchanged. The reweighting functions for the DY templates, f_{s} , f_{a} , and f_α respectively, are:

$$w_{\mathrm{s}}(|c_*|) = \frac{1+c_*^2}{1+c_*^2+\alpha\,(1-c_*^2)}, \tag{7}$$

$$w_{\mathrm{a}}(c_*) = \frac{c_*}{1+c_*^2+\alpha\,(1-c_*^2)}, \text{ and} \tag{8}$$

$$w_\alpha(|c_*|) = \frac{1-c_*^2}{1+c_*^2+\alpha\,(1-c_*^2)}. \tag{9}$$

The denominator of the DY reweighting functions is determined for each event from distributions of simulated SM DY events that are binned in $\cos\theta^*$ and generator-level $|y|$. The α values in the denominator are determined by fitting the generator-level distributions of the simulated events. Finally, to avoid negative values in the antisymmetric template, f_{a}, a linear combination of f_{s} and f_{a} is used in the fit, defined by $f_\pm = \frac{f_{\mathrm{s}} \pm f_{\mathrm{a}}}{2}$.

For the templates corresponding to the two LQ terms, $f_{\mathrm{LQ(pure)}}$ and $f_{\mathrm{LQ(int)}}$, events are reweighted as functions of both c_* and $m_{\ell\ell}$. The reweighting functions are given by:

$$w_{\mathrm{LQ(pure)}}^{S,V}(c_*, m_{\ell\ell}) = \left(N_{\mathrm{pure}}^{S,V}(m_{\ell\ell}) \frac{(1\mp c_*)^2}{\left(1-c_*+\frac{2m_{\mathrm{LQ}}^2}{m_{\ell\ell}^2}\right)^2} \right) \frac{1}{N_{\mathrm{SM}}(m_{\ell\ell})(1+c_*^2)} \tag{10}$$

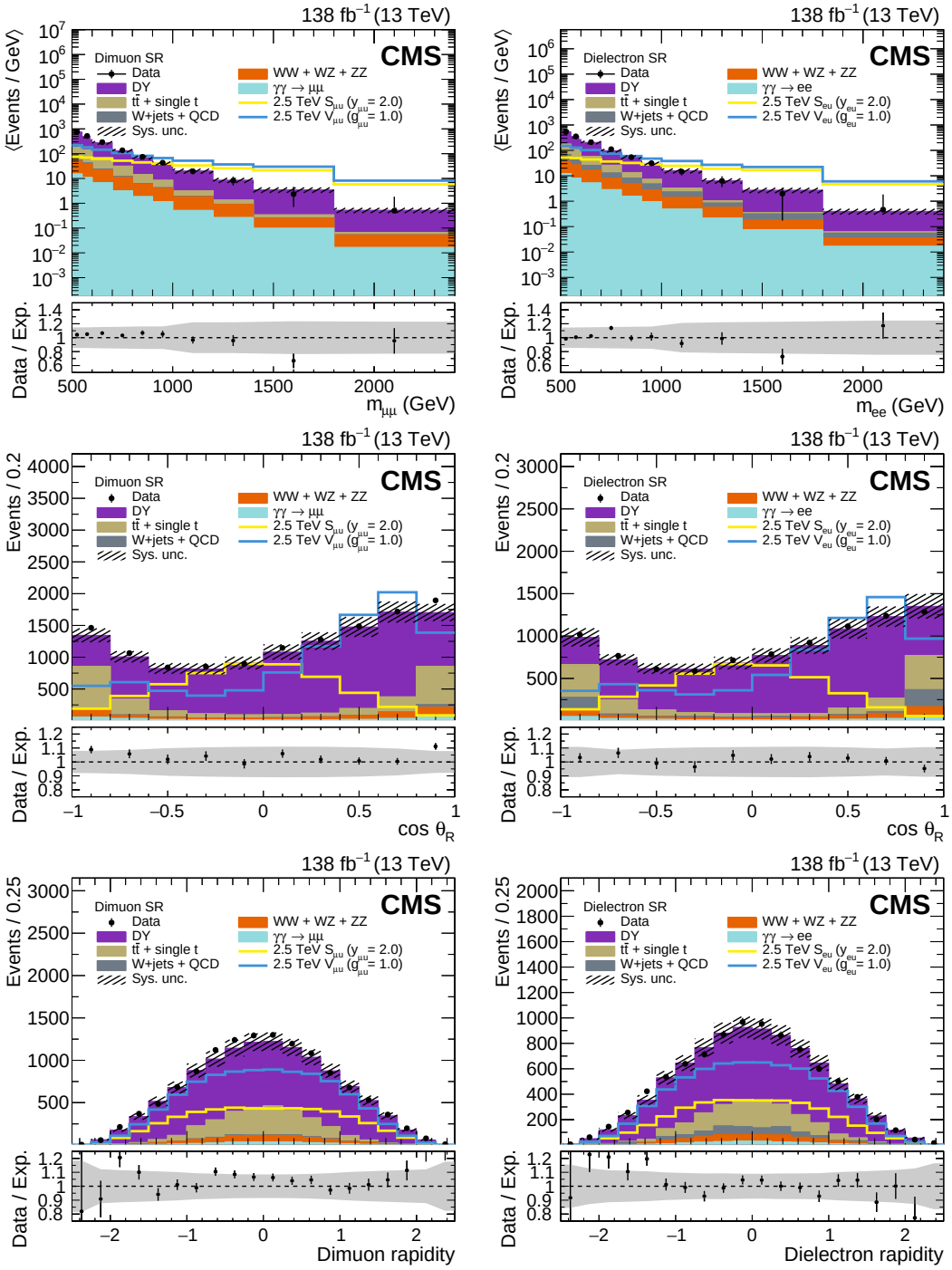


Figure 2: A comparison of data and expected background distributions in the dilepton invariant mass $m_{\ell\ell}$ (upper row), c_R (middle row), and dilepton rapidity (lower row). The distribution of $m_{\ell\ell}$ is shown as the average number of events per bin, whereas the distributions of c_R and rapidity are shown as the number of events per 0.2 in c_R and 0.25 in rapidity. The left (right) plots show the $\mu\mu$ (ee) channel. The blue histogram represents the signal yield of a hypothetical 2.5 TeV $S_{\mu u}$ (S_{eu}) with $y_{\mu u}$ (y_{eu}) = 2.0, while the yellow histogram represents the signal yield of a hypothetical 2.5 TeV $V_{\mu u}$ (V_{eu}) with $g_{\mu u}$ (g_{eu}) = 1.0. The black points with error bars represent the data and their statistical uncertainties. The background expectation is shown as stacked histograms. The hatched band shows the total systematic uncertainty in the expected background yield. The lower panels show the ratios of the data to the expectation. The gray bands represent the normalized uncertainty in the predicted yield. The error bars in the ratio plot represent the normalized statistical uncertainty in the data.

and

$$w^{S,V}_{\mathrm{LQ(int)}}(c_*, m_{\ell\ell}) = \left(N^{S,V}_{\mathrm{int}}(m_{\ell\ell}) \frac{(1 \mp c_*)^2}{\left(1 - c_* + \frac{2m^2_{\mathrm{LQ}}}{m^2_{\ell\ell}}\right)} \right) \frac{1}{N_{\mathrm{SM}}(m_{\ell\ell})(1 + c^2_*)}, \tag{11}$$

where S and V denote the scalar or vector case. The prefactors, $N^{S,V}_{\mathrm{pure/int}}(m_{\ell\ell})$, depend on the vector and axial-vector couplings of the quarks and leptons to the Z boson, as well as the quark charges. Thus, templates for an LQ coupled to a lepton and quark of specific flavors have different shapes compared to an LQ coupled to a different lepton and quark. The $N_{\mathrm{SM}}(m_{\ell\ell})$ prefactor represents the coefficient of the symmetric term $(1 + c^2_*)$ in the SM DY angular distribution. The denominators of the LQ reweighting functions are different from those of the SM DY functions, calculated from the analytical form of the LO SM DY cross section for each event. This is because the LQ modifies the $m_{\ell\ell}$ distribution, which must be taken into account in the reweighting.

The reweighting procedure described above has several benefits. The effects of misassigning the direction of the incident quark in the c_* computation, called the "dilution" effect, are accounted for correctly. Additionally, no dedicated MC samples need to be produced for the LQ process or its interference. The distribution of LQ events can be obtained by reweighting SM DY MC events using the analytical functional form of the LQ differential cross section.

The reweighting procedure was further validated by fitting LQ and DY templates at the generator level to simulated LQ signals using MADGRAPH5_aMC@NLO using the SLQRULES package [70]. Signals were generated at various mass points from 1–5 TeV. The fitted results agreed with the expected coupling values up to a maximum of 30% at $m_{\mathrm{LQ}} = 1$ TeV, decreasing with m_{LQ}. The discrepancy is attributable in part to the fact that the reweighting procedure does not account for NLO effects in the LQ exchange. We account for this in our fits by applying a 30% systematic uncertainty in the normalization of the LQ templates.

The total template for the scalar LQ case, binned in reconstructed $m_{\ell\ell}$, y, and c_{R}, is given by:

$$\begin{aligned} f_{\mathrm{data}} = & \sum_j f^j_{\mathrm{bkg}} + N(\alpha) \left(\alpha\, f_\alpha + \left(1 + \frac{3A_4}{8N}\right) f_+ + \left(1 - \frac{3A_4}{8N}\right) f_- \right) \\ & + y^4_{\mathrm{LQ}} f_{\mathrm{LQ(pure)}} + y^2_{\mathrm{LQ}} f_{\mathrm{LQ(int)}}, \end{aligned} \tag{12}$$

where f^j_{bkg} are templates for the non-DY backgrounds and $N(\alpha) = \frac{3}{4(2+\alpha)}$. The same template is used for the vector LQ case using the corresponding reweighting functions, and replacing y_{LQ} with g_{LQ}. The coefficients A_4, α, and either y^2_{LQ} or g^2_{LQ} are extracted in the fits to data.

Events are divided into bins based on $m_{\ell\ell}$, $|y|$, and c_{R}. For $m_{\ell\ell}$, three bins are used with bin edges at 500, 700, and 1000 GeV, with the third bin containing all events with $m_{\ell\ell} > 1000$ GeV. Three bins are defined for $|y|$, with edges at 0, 0.6, 1, and 2.4. The binning in c_{R} depends on the rapidity. Within the first rapidity bin, events are divided into eight bins in c_{R} of width 0.25. For the other two rapidity bins, events are divided into six bins in c_{R}, with edges of -1, -0.5, -0.25, 0, 0.25, 0.5, and 1. Bin edges were chosen after ensuring that there were sufficient simulated events in each bin, and fit uncertainties were minimized without losing precision.

Additional templates are created for the other background processes, with one template each for the MisID background, photon-induced dilepton production, DY $\tau\tau$ production, the combined top quark backgrounds ($\mathrm{t\bar{t}}$, tW), and the combined diboson backgrounds (WW, ZZ, WZ).

The top quark and MisID templates are symmetrized in c_R to reduce statistical fluctuations. The diboson, photon-induced dilepton, and DY $\tau\tau$ backgrounds are not symmetrized because of their significant inherent asymmetry.

8 Systematic uncertainties

Systematic uncertainties in the normalization and shapes of the templates arise from a variety of sources, and are incorporated in the fit to data through nuisance parameters in the likelihood. Systematic uncertainties affecting template normalizations are included using log-normal priors. For systematic uncertainties that change the shape of a template, shifted templates are constructed by varying the source of the systematic uncertainty up and down within its uncertainty. The uncertainties are incorporated into the likelihood by interpolation between the nominal and shifted templates, constrained with a Gaussian prior. Table 2 shows the impact of each uncertainty in the fitted LQ coupling for representative scalar and vector signal hypotheses.

Table 2: The contributions of the statistical uncertainty and of individual sources of systematic uncertainty to the total variance in the fitted value of y^2_{LQ} (g^2_{LQ}) for a scalar (vector) m_{LQ} of 2.5 TeV. For a given source of uncertainty, the impact is determined by fixing its associated nuisance parameter to the postfit value and evaluating the change in the total uncertainty. The quadrature sum of the uncertainties is approximately equal to the total uncertainty in y^2_{LQ} (g^2_{LQ}) for a scalar (vector) m_{LQ} of 2.5 TeV.

Source	Relative contribution (%)							
	y^2_{eu}	y^2_{ed}	$y^2_{\mu u}$	$y^2_{\mu d}$	g^2_{eu}	g^2_{ed}	$g^2_{\mu u}$	$g^2_{\mu d}$
Statistical uncertainty	84	84	81	79	34	33	25	32
LQ LO reweighting	21	31	27	25	28	27	53	37
MC and MisID backgrounds statistical uncertainty	15	15	14	16	35	56	31	46
α_S + renormalization/factorization scales	7	11	20	22	15	19	28	32
eμ shape corrections	7	8	17	16	11	4	16	11
Background cross sections	12	14	33	36	23	22	54	48
Integrated luminosity	13	13	20	23	19	19	32	38
Pileup	6.9	6.4	9.5	8.8	5.1	5.7	5.1	6.0
PDFs	6.0	6.9	7.1	8.2	8.8	4.6	11	8.8
Trigger efficiency	11	9.0	2.5	1.3	19	7.1	4.3	6.3
Lepton momentum scale	17	22	5.7	3.1	30	12	14	6.9
Lepton identification/isolation	33	20	9.9	10	62	57	12	16
MisID shape & normalization	17	19	15	16	38	58	31	47

A significant source of uncertainty is due to the creation of the LQ signal templates using LO reweighting of NLO DY MC events. A normalization uncertainty of 30% in the coupling is assigned to the pure and interference LQ templates. This uncertainty is based on bias tests performed on simulations with injected signal events that were generated with MADGRAPH5_aMC@NLO following Ref. [70]. This uncertainty does not affect the shape of the templates.

Several sources of systematic uncertainty are due to the modeling of leptons in simulation. These include uncertainties in the momentum scale, the efficiency of the reconstruction and identification criteria, and the trigger efficiency. These uncertainties are small for the muon

channel, but are dominant in the electron channel.

Additional systematic uncertainties are applied to templates estimated from simulation. The uncertainty in the PDFs is assigned from the Hessian variations of the PDF sets. Uncertainties due to missing higher-order contributions are estimated by varying the renormalization and factorization scales independently by factors of two. Additional uncertainties are assigned to the cross sections of the DY, $\mathrm{t\bar{t}}$, and diboson processes based on comparisons between generators, of size 3, 5, and 4%, respectively. Similarly, an uncertainty of 6% is assigned to the normalization of the $\gamma\gamma \to \ell\ell$ process, based on a comparison between the Suri–Yennie structure functions and the LuxQED photon PDFs [77, 78]. The statistical uncertainties due to the limited number of MC events are implemented using the simplified Barlow–Beeston approach [79]. Since the bin contents of $\pm c_*$ are correlated because each event is used twice, each pair of $\pm c_*$ bins is varied together and accounts for a separate nuisance parameter.

The MisID background is assigned a normalization uncertainty of 50% based on closure studies of the misidentification rate in simulation and a shape uncertainty based on the difference between the MisID estimate in SS and OS events. The MisID uncertainty primarily affects the electron channel, given the higher rate of misidentified electrons than muons.

The $\mathrm{t\bar{t}}$ and diboson templates are assigned a shape uncertainty due to the correction to the c_R distributions derived from $\mathrm{e}\mu$ events. The integrated luminosities for the 2016, 2017, and 2018 data-taking years have 1.2–2.5% individual uncertainties [80–82], while the overall uncertainty for the 2016–2018 period is 1.6%. Small uncertainties in the modeling of pileup are also incorporated.

The uncertainties in the PDFs, pileup, electron and muon efficiencies, MC cross sections, luminosity, and the LQ template normalization are correlated for all the three data-taking years. The $\mathrm{e}\mu$ shape corrections, and renormalization and factorization scale corrections are correlated for the 2017 and 2018 periods. The rest are treated independently per year. In the results for the scalar LQ couplings, the contribution of statistical uncertainties is larger than the systematic uncertainties. However for the vector LQ couplings, the systematic uncertainties have a larger contribution. This is because of the differences in shapes between the scalar and vector LQ templates.

Table 2 shows that the largest contributors to the uncertainties in $y^2_{\mu\mathrm{u}}$, $y^2_{\mu\mathrm{d}}$, $g^2_{\mu\mathrm{u}}$, and $g^2_{\mu\mathrm{d}}$ are those arising from the LO reweighting scheme, the renormalization and factorization scales, and the background cross sections. Additionally, the electron identification and isolation has major contributions to the uncertainties in y^2_{eu}, y^2_{ed}, g^2_{eu}, and g^2_{ed}. The post-fit up and down variations of these systematic uncertainties are asymmetric in their impacts on the LQ couplings. This is because the likelihood function for each model is asymmetric in y^2_LQ (g^2_LQ), and not quadratic. The shapes of the likelihoods follow from Eqs. (4) and (5). For each LQ model considered, the prefactor $N^{S(V)}_\mathrm{int}$ can assume positive or negative values based on the fermions involved in the LQ exchange, leading to constructive or destructive interference. Accordingly, combinations of the pure LQ exchange term and the LQ-SM interference term result in asymmetric likelihoods, that become highly nonquadratic for large couplings.

9 Results

Template fits are performed to the data for each LQ signal hypothesis, following Eq. (12). The COMBINE package [83] is used to perform maximum likelihood fits to the data. A range of positive and negative values of y^2_LQ (g^2_LQ) is floated in the fit in order to ensure fit stability. The

extracted best fit parameters for a candidate m_{LQ} of 2.5 TeV are shown in Tables 3 and 4. The corresponding upper and lower bounds of the Feldman–Cousins intervals [84] for y^2_{LQ} (g^2_{LQ}) are reported as well. In the SM, the expected value of A_0 is 0.05, and that of A_4 is 1.61. These quantities were measured more precisely in Ref. [36]. The best fit values for g^2_{ed} and $g^2_{\mu\mathrm{d}}$ are positive, while the others are negative. This is due to the destructive interference between LQ and SM amplitudes for V_{ed} and $\mathrm{V}_{\mu\mathrm{d}}$ exchanges, and constructive interference in the other models. All results are found to be consistent with the SM background expectations. The fit results are shown in Figs. 3–6. In each figure, the overall signal yield is scaled by -10 because the sum of the pure and interference contributions scaled by the post-fit values of y^4_{LQ} (g^4_{LQ}) and y^2_{LQ} (g^2_{LQ}) is negative.

Limits at 95% CL are set on the absolute value of the LQ-fermion couplings as a function of the m_{LQ} for each coupling and spin hypothesis. The limit-setting procedure employs a modified frequentist approach based on the $\mathrm{CL_s}$ criterion [85, 86], using an asymptotic approximation for the distribution of the test statistic [87]. Limits extracted with this approach are nearly identical to those obtained from the Feldman–Cousins method. The limits are shown in Figs. 7 and 8 for the scalar case, and Figs. 9 and 10 for the vector case, assuming branching fractions of 100% for each channel.

In general, for equal coupling values, the cross sections for vector LQ production are larger than for scalar LQ production, hence the limits on $|g_{\mathrm{LQ}}|$ are generally stronger than those on $|y_{\mathrm{LQ}}|$. The limits on up-type couplings are stronger than the limits on down-type couplings because of the larger up quark content of the proton. In the V_{ed} and $\mathrm{V}_{\mu\mathrm{d}}$ cases, the interference process is negative, and the likelihood functions for these models are thus quite asymmetric and nonquadratic. This leads to smaller cross sections and weaker expected and observed limits than the other cases. The uncertainties in the expected limits are also accordingly larger than in the other cases. Further, the observed limit on $|g_{\mathrm{ed}}|$ is more stringent than the expected limit, despite the positive best fit value for the V_{ed} mass of 2.5 TeV, as shown in Table 4. This stems from the asymmetric nuisance impacts arising from the nonquadraticity in the likelihood, as discussed in Section 8.

At $m_{\mathrm{LQ}} \gg m_{\ell\ell}$, the cross section scales as $y^2_{\mathrm{LQ}}/m^2_{\mathrm{LQ}}$ ($g^2_{\mathrm{LQ}}/m^2_{\mathrm{LQ}}$), leading to the linearly increasing limits that are observed. Coupling values larger than 4π are nonperturbative.

For the scalar case, coupling values of 0.4–1.1 (0.3–1.0) are excluded for LQs coupled to electrons (muons) with masses between 1–5 TeV. These limits significantly extend the previous best limits from single production [24], which excluded S_{eu} and S_{ed} masses up to 1.7 TeV depending on the coupling, and pair production [25], which excluded S_{eu} and S_{ed} masses up to 1.4 TeV independent of the mass. Similarly, for the vector case, coupling values of 0.2–0.5 (0.1–0.4) are excluded for LQs coupled to electrons (muons). These are the first limits on vector LQs coupled to first- and second-generation fermions obtained via nonresonant t-channel exchange, extending the sensitivity of previous searches.

10 Summary

A search for the t-channel exchange of leptoquarks (LQs) coupled to first- and second-generation fermions has been presented. The search uses proton-proton collision data at $\sqrt{s} = 13$ TeV, corresponding to an integrated luminosity of 138 fb^{-1}. Both scalar and vector LQs are considered, with masses between 1 and 5 TeV, for exclusive LQ couplings to an up or a down quark and a muon or an electron. The t-channel exchange of an LQ modifies the dilepton

Table 3: Best fit values of A_0, A_4, and y^2_{LQ} for scalar LQ models. The Feldman–Cousins confidence interval for y^2_{LQ} is shown at 68% CL. Results are shown for a candidate m_{LQ} of 2.5 TeV.

Model	A_0	A_4	y^2_{LQ}	Lower bound on y^2_{LQ}	Upper bound on y^2_{LQ}
$\mathrm{S}_{\mu\mathrm{u}}$	0.02 ± 0.06	1.59 ± 0.07	$-0.13^{+0.14}_{-0.15}\,(\mathrm{stat})^{+0.06}_{-0.11}\,(\mathrm{syst})$	0	0.082
$\mathrm{S}_{\mu\mathrm{d}}$	0.02 ± 0.06	1.60 ± 0.07	$-0.11^{+0.18}_{-0.20}\,(\mathrm{stat})^{+0.09}_{-0.13}\,(\mathrm{syst})$	0	0.119
S_{eu}	0.07 ± 0.07	1.61 ± 0.08	$-0.10^{+0.15}_{-0.17}\,(\mathrm{stat})^{+0.07}_{-0.11}\,(\mathrm{syst})$	0	0.093
S_{ed}	0.07 ± 0.07	1.62 ± 0.08	$-0.09^{+0.20}_{-0.23}\,(\mathrm{stat})^{+0.11}_{-0.13}\,(\mathrm{syst})$	0	0.138

Table 4: Best fit values of A_0, A_4, and g^2_{LQ} for vector LQ models. The Feldman–Cousins confidence interval for g^2_{LQ} is shown at 68% CL. Results are shown for a candidate m_{LQ} of 2.5 TeV.

Model	A_0	A_4	g^2_{LQ}	Lower bound on g^2_{LQ}	Upper bound on g^2_{LQ}
$\mathrm{V}_{\mu\mathrm{u}}$	0.01 ± 0.05	1.63 ± 0.06	$-0.10^{+0.02}_{-0.02}\,(\mathrm{stat})^{+0.04}_{-0.08}\,(\mathrm{syst})$	0	0.029
$\mathrm{V}_{\mu\mathrm{d}}$	0.01 ± 0.05	1.61 ± 0.06	$0.14^{+0.05}_{-0.05}\,(\mathrm{stat})^{+0.14}_{-0.07}\,(\mathrm{syst})$	0.036	0.328
V_{eu}	0.05 ± 0.07	1.66 ± 0.08	$-0.09^{+0.03}_{-0.03}\,(\mathrm{stat})^{+0.04}_{-0.08}\,(\mathrm{syst})$	0	0.026
V_{ed}	0.06 ± 0.07	1.64 ± 0.08	$0.13^{+0.06}_{-0.06}\,(\mathrm{stat})^{+0.17}_{-0.09}\,(\mathrm{syst})$	0.038	0.352

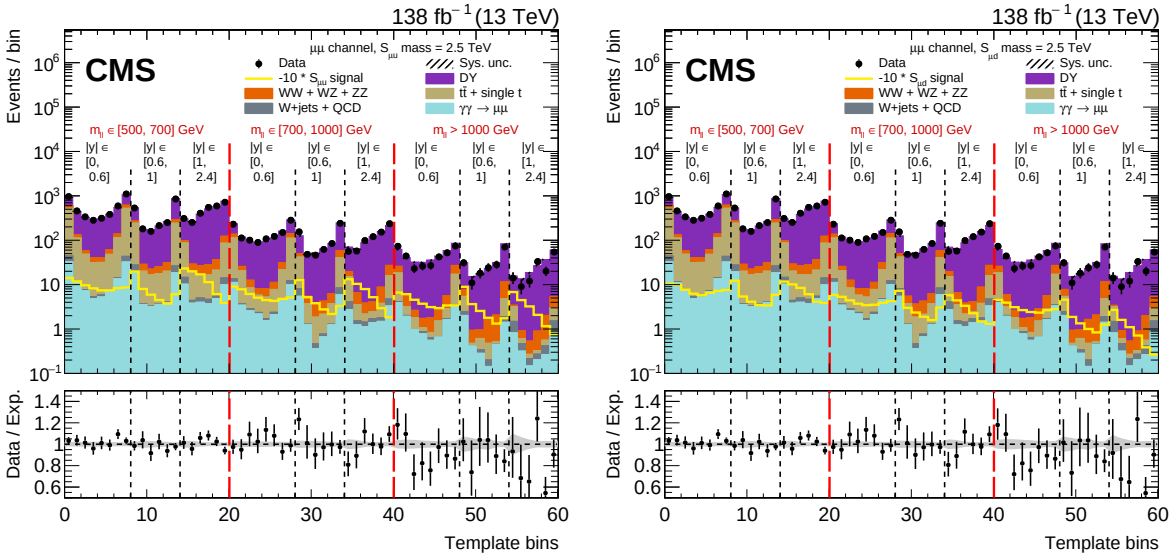


Figure 3: The observed data in the dimuon channel and the fitted signal-plus-background templates, shown for the $\mathrm{S}_{\mu\mathrm{u}}$ (left) and $\mathrm{S}_{\mu\mathrm{d}}$ (right) scenarios with a candidate m_{LQ} of 2.5 TeV. The black points are the observed data, the stacked histograms represent the backgrounds, and the yellow histogram shows the fitted LQ signal scaled by -10. Distributions of events are binned in the reconstructed $m_{\ell\ell}$ (vertical red dashed lines), $|y|$ (vertical black dashed lines), and c_{R} (Section 7). The lower panels show the ratios of the data to the expectation. The gray bands represent the normalized uncertainty in the predicted yield. The error bars in the ratio plot represent the normalized statistical uncertainty in the data.

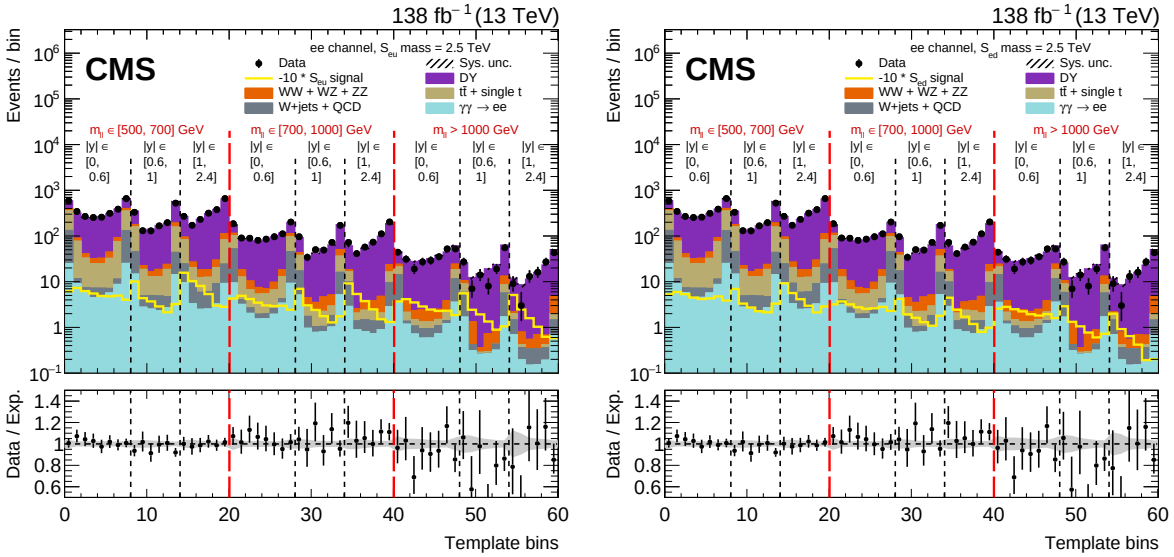


Figure 4: The observed data in the dielectron channel and the fitted signal-plus-background templates, shown for the S_{eu} (left) and S_{ed} (right) scenarios with a candidate m_{LQ} of 2.5 TeV. The black points are the observed data, the stacked histograms represent the backgrounds, and the yellow histogram shows the fitted LQ signal scaled by -10. Distributions of events are binned in the reconstructed $m_{\ell\ell}$ (vertical red dashed lines), $|y|$ (vertical black dashed lines), and c_R (Section 7). The lower panels show the ratios of the data to the expectation. The gray bands represent the normalized uncertainty in the predicted yield. The error bars in the ratio plot represent the normalized statistical uncertainty in the data.

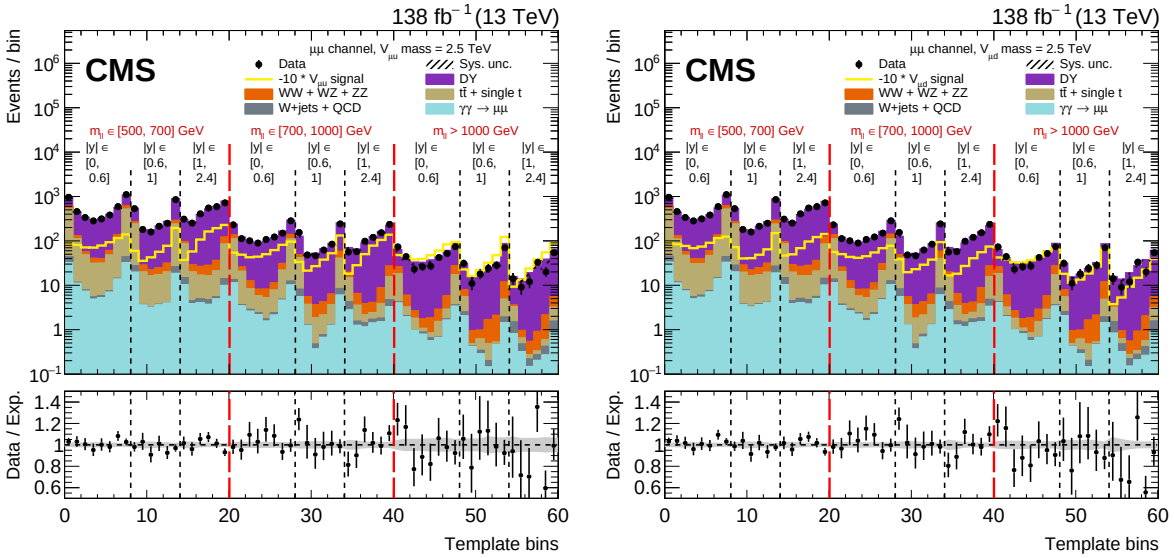


Figure 5: The observed data in the dimuon channel and the fitted signal-plus-background templates, shown for the $V_{\mu u}$ (left) and $V_{\mu d}$ (right) scenario with a candidate m_{LQ} of 2.5 TeV. The black points are the observed data, the stacked histograms represent the backgrounds, and the yellow histogram shows the fitted LQ signal scaled by -10. Distributions of events are binned in the reconstructed $m_{\ell\ell}$ (vertical red dashed lines), $|y|$ (vertical black dashed lines), and c_R (Section 7). The lower panels show the ratios of the data to the expectation. The gray bands represent the normalized uncertainty in the predicted yield. The error bars in the ratio plot represent the normalized statistical uncertainty in the data.

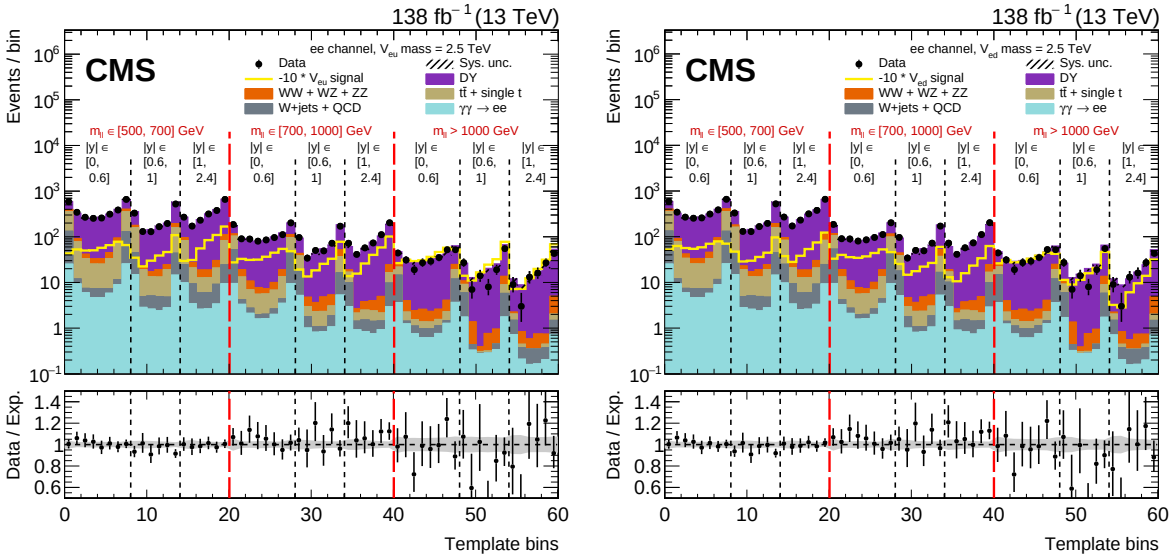


Figure 6: The observed data in the dielectron channel and the fitted signal-plus-background templates, shown for the V_{eu} (left) and V_{ed} (right) scenario with a candidate m_{LQ} of 2.5 TeV. The black points are the observed data, the stacked histograms represent the backgrounds, and the yellow histogram shows the fitted LQ signal scaled by -10. Distributions of events are binned in the reconstructed $m_{\ell\ell}$ (vertical red dashed lines), $|y|$ (vertical black dashed lines), and c_R (Section 7). The lower panels show the ratios of the data to the expectation. The gray bands represent the normalized uncertainty in the predicted yield. The error bars in the ratio plot represent the normalized statistical uncertainty in the data.

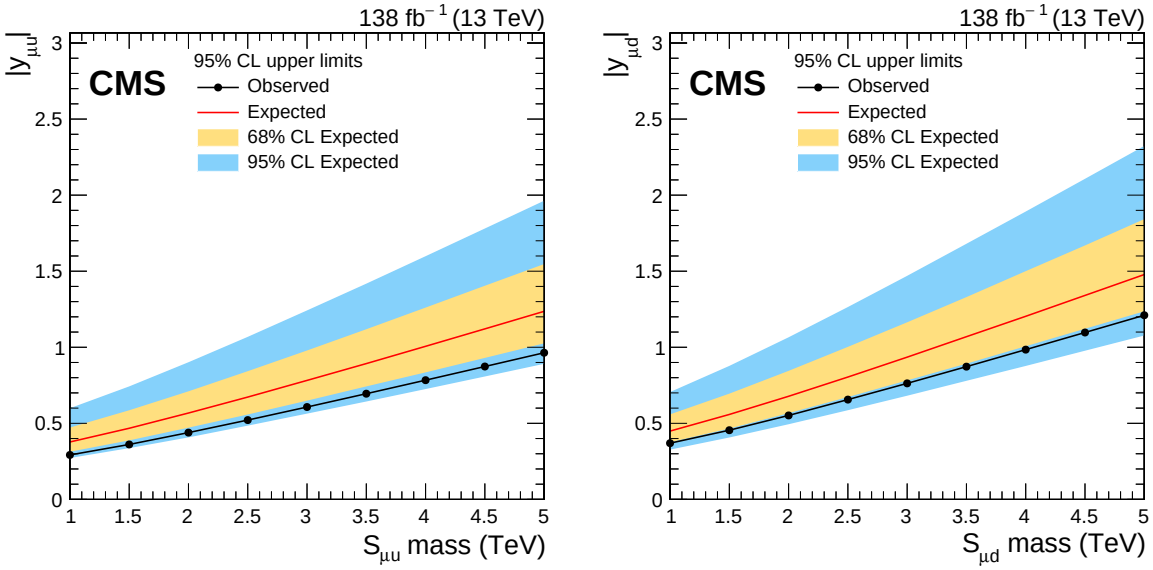


Figure 7: Upper limits at 95% CL on the LQ-fermion couplings, $|y_{\mu u}|$ (left) and $|y_{\mu d}|$ (right), as a function of m_{LQ} for scalar LQs coupled to muons. The black points show the observed limits, the red line shows the expected limits, and the yellow and blue bands show the variations on the expected limit at 68% and 95% CL, respectively.

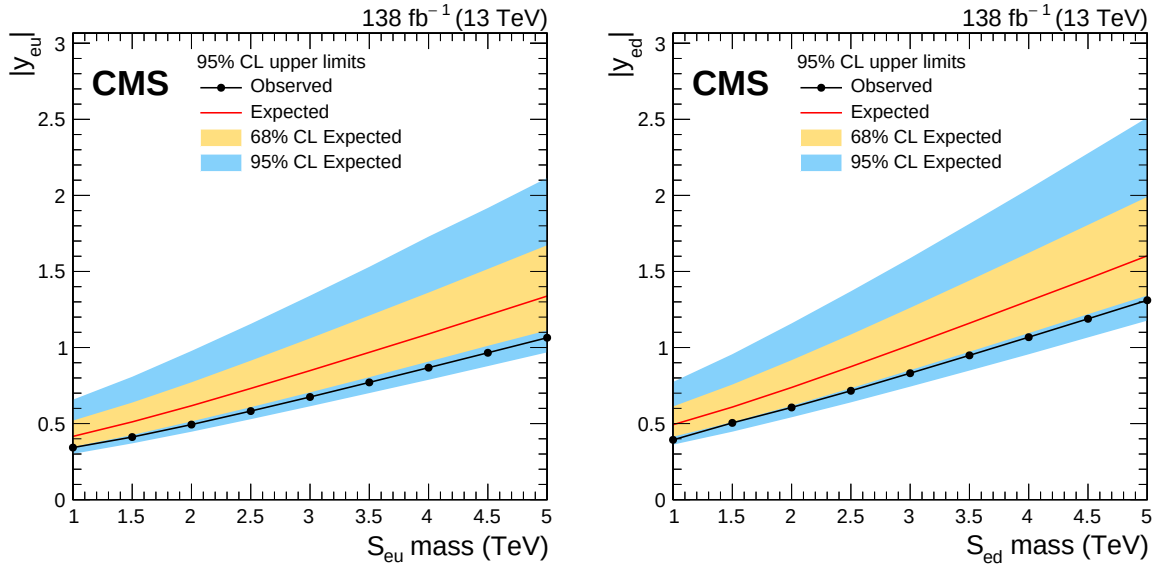


Figure 8: Upper limits at 95% CL on the LQ-fermion couplings, $|y_{eu}|$ (left) and $|y_{ed}|$ (right), as a function of m_{LQ} for scalar LQs coupled to electrons. The black points show the observed limits, the red line shows the expected limits, and the yellow and blue bands show the variations on the expected limit at 68% and 95% CL, respectively.

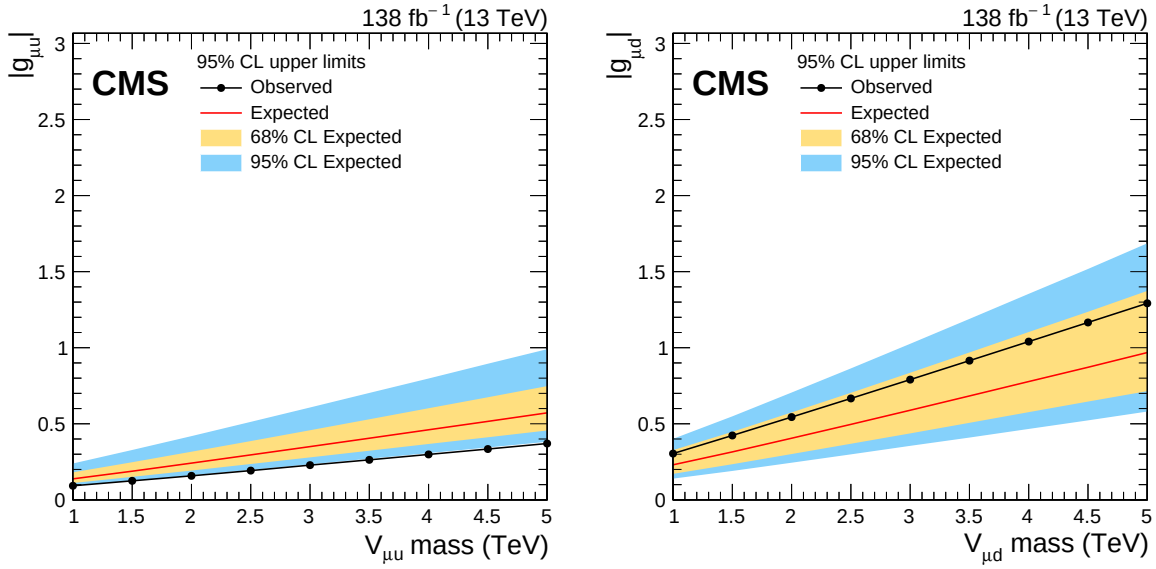


Figure 9: Upper limits at 95% CL on the LQ-fermion couplings, $|g_{\mu u}|$ (left) and $|g_{\mu d}|$ (right), as a function of m_{LQ} for vector LQs coupled to muons. The black points show the observed limits, the red line shows the expected limits, and the yellow and blue bands show the variations on the expected limit at 68% and 95% CL, respectively.

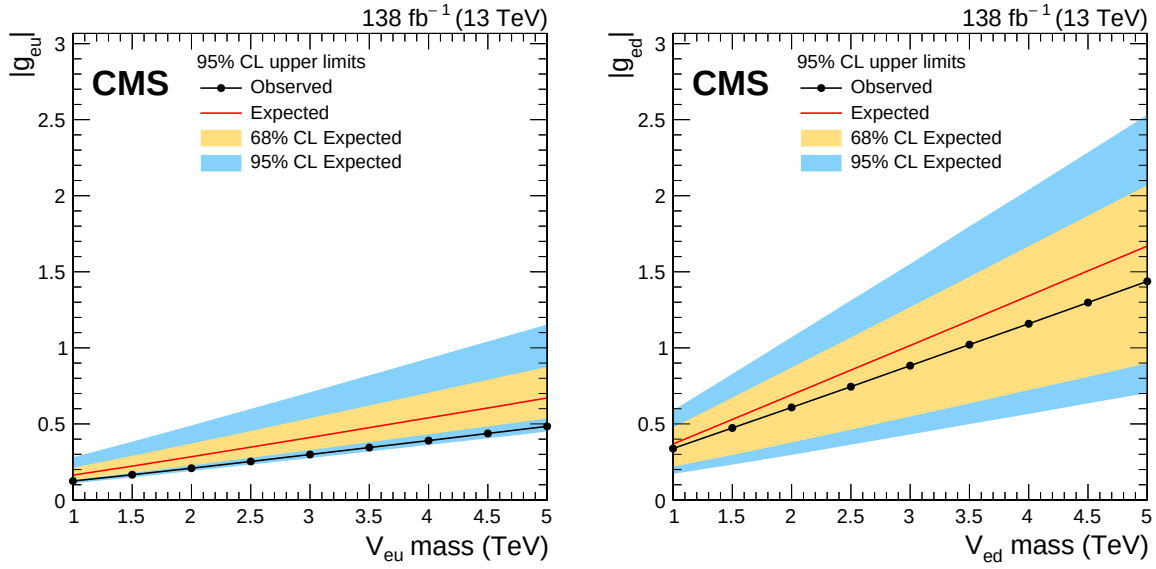


Figure 10: Upper limits at 95% CL on the LQ-fermion couplings, $|g_{eu}|$ (left) and $|g_{ed}|$ (right), as a function of m_{LQ} for vector LQs coupled to electrons. The black points show the observed limits, the red line shows the expected limits, and the yellow and blue bands show the variations on the expected limit at 68% and 95% CL, respectively.

angular distributions at masses well below the resonance mass of the LQ. A template fit to the angular and invariant mass distributions of high-mass dilepton events is used to distinguish the signal process from the dominant Drell–Yan background, incorporating the interference effects. No evidence for such LQs is observed. Limits are set at 95% confidence level on the LQ-fermion couplings. For scalar LQs with masses in the 1–5 TeV range, coupling values greater than 0.4–1.3 (0.3–1.0) are excluded for LQs coupled to a muon or an electron, and an up (down) quark, and couplings greater than 0.3–1.4 (0.1–0.5) are excluded for the respective vector LQs. This search is sensitive to LQs with significantly higher masses than prior single- and pair-production searches, establishing stringent limits on LQs with masses up to 5 TeV.

Acknowledgments

We congratulate our colleagues in the CERN accelerator departments for the excellent performance of the LHC and thank the technical and administrative staffs at CERN and at other CMS institutes for their contributions to the success of the CMS effort. In addition, we gratefully acknowledge the computing centers and personnel of the Worldwide LHC Computing Grid and other centers for delivering so effectively the computing infrastructure essential to our analyses. Finally, we acknowledge the enduring support for the construction and operation of the LHC, the CMS detector, and the supporting computing infrastructure provided by the following funding agencies: SC (Armenia), BMBWF and FWF (Austria); FNRS and FWO (Belgium); CNPq, CAPES, FAPERJ, FAPERGS, and FAPESP (Brazil); MES and BNSF (Bulgaria); CERN; CAS, MoST, and NSFC (China); MINCIENCIAS (Colombia); MSES and CSF (Croatia); RIF (Cyprus); SENESCYT (Ecuador); ERC PRG, RVTT3 and MoER TK202 (Estonia); Academy of Finland, MEC, and HIP (Finland); CEA and CNRS/IN2P3 (France); SRNSF (Georgia); BMBF, DFG, and HGF (Germany); GSRI (Greece); NKFIH (Hungary); DAE and DST (India); IPM (Iran); SFI (Ireland); INFN (Italy); MSIP and NRF (Republic of Korea); MES (Latvia); LMTLT (Lithuania); MOE and UM (Malaysia); BUAP, CINVESTAV, CONACYT, LNS, SEP, and UASLP-FAI (Mexico); MOS (Montenegro); MBIE (New Zealand); PAEC (Pakistan); MES and

NSC (Poland); FCT (Portugal); MESTD (Serbia); MICIU/AEI and PCTI (Spain); MOSTR (Sri Lanka); Swiss Funding Agencies (Switzerland); MST (Taipei); MHESI and NSTDA (Thailand); TUBITAK and TENMAK (Turkey); NASU (Ukraine); STFC (United Kingdom); DOE and NSF (USA).

Individuals have received support from the Marie-Curie program and the European Research Council and Horizon 2020 Grant, contract Nos. 675440, 724704, 752730, 758316, 765710, 824093, 101115353, 101002207, and COST Action CA16108 (European Union); the Leventis Foundation; the Alfred P. Sloan Foundation; the Alexander von Humboldt Foundation; the Science Committee, project no. 22rl-037 (Armenia); the Fonds pour la Formation à la Recherche dans l'Industrie et dans l'Agriculture (FRIA-Belgium); the Beijing Municipal Science & Technology Commission, No. Z191100007219010 and Fundamental Research Funds for the Central Universities (China); the Ministry of Education, Youth and Sports (MEYS) of the Czech Republic; the Shota Rustaveli National Science Foundation, grant FR-22-985 (Georgia); the Deutsche Forschungsgemeinschaft (DFG), among others, under Germany's Excellence Strategy – EXC 2121 "Quantum Universe" – 390833306, and under project number 400140256 - GRK2497; the Hellenic Foundation for Research and Innovation (HFRI), Project Number 2288 (Greece); the Hungarian Academy of Sciences, the New National Excellence Program - ÚNKP, the NKFIH research grants K 131991, K 133046, K 138136, K 143460, K 143477, K 146913, K 146914, K 147048, 2020-2.2.1-ED-2021-00181, TKP2021-NKTA-64, and 2021-4.1.2-NEMZ_KI-2024-00036 (Hungary); the Council of Science and Industrial Research, India; ICSC – National Research Center for High Performance Computing, Big Data and Quantum Computing and FAIR – Future Artificial Intelligence Research, funded by the NextGenerationEU program (Italy); the Latvian Council of Science; the Ministry of Education and Science, project no. 2022/WK/14, and the National Science Center, contracts Opus 2021/41/B/ST2/01369 and 2021/43/B/ST2/01552 (Poland); the Fundação para a Ciência e a Tecnologia, grant CEECIND/01334/2018 (Portugal); the National Priorities Research Program by Qatar National Research Fund; MICIU/AEI/10.13039/501100011033, ERDF/EU, "European Union NextGenerationEU/PRTR", and Programa Severo Ochoa del Principado de Asturias (Spain); the Chulalongkorn Academic into Its 2nd Century Project Advancement Project, and the National Science, Research and Innovation Fund via the Program Management Unit for Human Resources & Institutional Development, Research and Innovation, grant B39G670016 (Thailand); the Kavli Foundation; the Nvidia Corporation; the SuperMicro Corporation; the Welch Foundation, contract C-1845; and the Weston Havens Foundation (USA).

References

[1] J. C. Pati and A. Salam, "Lepton number as the fourth color", *Phys. Rev. D* **10** (1974) 275, doi:10.1103/PhysRevD.10.275. [Erratum: doi:10.1103/PhysRevD.11.703.2].

[2] H. Georgi and S. L. Glashow, "Unity of all elementary particle forces", *Phys. Rev. Lett.* **32** (1974) 438, doi:10.1103/PhysRevLett.32.438.

[3] G. Senjanovic and A. Sokorac, "Light Leptoquarks in SO(10)", *Z. Phys. C* **20** (1983) 255, doi:10.1007/BF01574858.

[4] S. Davidson and S. Descotes-Genon, "Minimal flavour violation for leptoquarks", *JHEP* **11** (2010) 073, doi:10.1007/JHEP11(2010)073, arXiv:1009.1998.

[5] I. Dorsner and P. Fileviez Perez, "Unification without supersymmetry: Neutrino mass, proton decay and light leptoquarks", *Nucl. Phys. B* **723** (2005) 53, doi:10.1016/j.nuclphysb.2005.06.016, arXiv:hep-ph/0504276.

[6] W. Buchmuller and D. Wyler, "Constraints on SU(5) type leptoquarks", *Phys. Lett. B* **177** (1986) 377, doi:10.1016/0370-2693(86)90771-9.

[7] B. Gripaios, M. Nardecchia, and S. A. Renner, "Composite leptoquarks and anomalies in *b*-meson decays", *JHEP* **05** (2015) 006, doi:10.1007/JHEP05(2015)006, arXiv:1412.1791.

[8] B. Gripaios, "Composite leptoquarks at the LHC", *JHEP* **02** (2010) 045, doi:10.1007/JHEP02(2010)045, arXiv:0910.1789.

[9] E. Farhi and L. Susskind, "Technicolor", *Phys. Rept.* **74** (1981) 277, doi:10.1016/0370-1573(81)90173-3.

[10] S. Dimopoulos, "Technicolored signatures", *Nucl. Phys. B* **168** (1980) 69, doi:10.1016/0550-3213(80)90277-1.

[11] B. Schrempp and F. Schrempp, "Light leptoquarks", *Phys. Lett. B* **153** (1985) 101, doi:10.1016/0370-2693(85)91450-9.

[12] M. J. Baker et al., "The coannihilation codex", *JHEP* **12** (2015) 120, doi:10.1007/JHEP12(2015)120, arXiv:1510.03434.

[13] S.-M. Choi, Y.-J. Kang, H. M. Lee, and T.-G. Ro, "Lepto-Quark portal dark matter", *JHEP* **10** (2018) 104, doi:10.1007/JHEP10(2018)104, arXiv:1807.06547.

[14] R. Barbier et al., "R-parity violating supersymmetry", *Phys. Rept.* **420** (2005) 1, doi:10.1016/j.physrep.2005.08.006, arXiv:hep-ph/0406039.

[15] Muon $g-2$ Collaboration, "Measurement of the positive muon anomalous magnetic moment to 0.46 ppm", *Phys. Rev. Lett.* **126** (2021) 141801, doi:10.1103/PhysRevLett.126.141801, arXiv:2104.03281.

[16] S. Borsanyi et al., "Leading hadronic contribution to the muon magnetic moment from lattice QCD", *Nature* **593** (2021) 51, doi:10.1038/s41586-021-03418-1, arXiv:2002.12347.

[17] I. Doršner, S. Fajfer, and O. Sumensari, "Muon $g-2$ and scalar leptoquark mixing", *JHEP* **06** (2020) 089, doi:10.1007/JHEP06(2020)089, arXiv:1910.03877.

[18] Muon $g-2$ Collaboration, "Measurement of the positive muon anomalous magnetic moment to 127 ppb", 2025. arXiv:2506.03069.

[19] I. Doršner et al., "Physics of leptoquarks in precision experiments and at particle colliders", *Phys. Rept.* **641** (2016) 1, doi:10.1016/j.physrep.2016.06.001, arXiv:1603.04993.

[20] CMS Collaboration, "Search for a third-generation leptoquark coupled to a τ lepton and a b quark through single, pair, and nonresonant production in proton-proton collisions at $\sqrt{s}$ = 13 TeV", *JHEP* **05** (2024) 311, doi:10.1007/JHEP05(2024)311, arXiv:2308.07826.

[21] ATLAS Collaboration, "Search for pair production of third-generation leptoquarks decaying into a bottom quark and a τ-lepton with the ATLAS detector", *Eur. Phys. J. C* **83** (2023) 1075, doi:10.1140/epjc/s10052-023-12104-7, arXiv:2303.01294.

[22] CMS Collaboration, "Searches for additional Higgs bosons and for vector leptoquarks in $\tau\tau$ final states in proton-proton collisions at $\sqrt{s}$ = 13 TeV", *JHEP* **07** (2023) 073, doi:10.1007/JHEP07(2023)073, arXiv:2208.02717.

[23] ATLAS Collaboration, "Search for pairs of scalar leptoquarks decaying into quarks and electrons or muons in $\sqrt{s}$ = 13 TeV pp collisions with the ATLAS detector", *JHEP* **10** (2020) 112, doi:10.1007/JHEP10(2020)112, arXiv:2006.05872.

[24] CMS Collaboration, "Search for single production of scalar leptoquarks in proton-proton collisions at $\sqrt{s} = 8$ TeV", *Phys. Rev. D* **93** (2016) 032005, doi:10.1103/PhysRevD.93.032005, arXiv:1509.03750. [Erratum: doi:10.1103/PhysRevD.95.039906].

[25] CMS Collaboration, "Search for pair production of first-generation scalar leptoquarks at $\sqrt{s} = 13$ TeV", *Phys. Rev. D* **99** (2019) 052002, doi:10.1103/PhysRevD.99.052002, arXiv:1811.01197.

[26] CMS Collaboration, "Search for pair production of second-generation leptoquarks at $\sqrt{s} = 13$ TeV", *Phys. Rev. D* **99** (2019) 032014, doi:10.1103/PhysRevD.99.032014, arXiv:1808.05082.

[27] CMS Collaboration, "Search for pair production of first and second generation leptoquarks in proton-proton collisions at $\sqrt{s}$ = 8 TeV", *Phys. Rev. D* **93** (2016) 032004, doi:10.1103/PhysRevD.93.032004, arXiv:1509.03744.

[28] N. Raj, "Anticipating nonresonant new physics in dilepton angular spectra at the LHC", *Phys. Rev. D* **95** (2017) 015011, doi:10.1103/PhysRevD.95.015011, arXiv:1610.03795.

[29] A. Crivellin, D. Müller, and L. Schnell, "Combined constraints on first generation leptoquarks", *Phys. Rev. D* **103** (2021) 115023, doi:10.1103/PhysRevD.103.115023, arXiv:2104.06417. [Addendum: doi:10.1103/PhysRevD.104.055020].

[30] I. Bigaran and R. R. Volkas, "Getting chirality right: Single scalar leptoquark solutions to the $(g-2)_{e,\mu}$ puzzle", *Phys. Rev. D* **102** (2020) 075037, doi:10.1103/PhysRevD.102.075037, arXiv:2002.12544.

[31] I. Dorsner, "Novel leptoquark pair production @LHC", *PoS* **CORFU2022** (2023) 111, doi:10.22323/1.436.0111.

[32] D. J. Robinson, B. Shakya, and J. Zupan, "Right-handed neutrinos and R(D*)", *JHEP* **02** (2019) 119, doi:10.1007/JHEP02(2019)119, arXiv:1807.04753.

[33] D. Bečirević, N. Košnik, O. Sumensari, and R. Zukanovich Funchal, "Palatable leptoquark scenarios for lepton flavor violation in exclusive $b \to s\ell_1\ell_2$ modes", *JHEP* **11** (2016) 035, doi:10.1007/JHEP11(2016)035, arXiv:1608.07583.

[34] HEPData record for this analysis, 2024. doi:10.17182/hepdata.156848.

[35] J. C. Collins and D. E. Soper, "Angular distribution of dileptons in high-energy hadron collisions", *Phys. Rev. D* **16** (1977) 2219, doi:10.1103/PhysRevD.16.2219.

[36] CMS Collaboration, "Measurement of the Drell-Yan forward-backward asymmetry at high dilepton masses in proton-proton collisions at $\sqrt{s}$ = 13 TeV", *JHEP* **08** (2022) 063, doi:10.1007/JHEP08(2022)063, arXiv:2202.12327.

[37] E. Mirkes, "Angular decay distribution of leptons from W bosons at NLO in hadronic collisions", *Nucl. Phys. B* **387** (1992) 3, doi:10.1016/0550-3213(92)90046-E.

[38] E. Mirkes and J. Ohnemus, "Angular distributions of Drell-Yan lepton pairs at the Tevatron: Order $\alpha - s^2$ corrections and Monte Carlo studies", *Phys. Rev. D* **51** (1995) 4891, doi:10.1103/PhysRevD.51.4891, arXiv:hep-ph/9412289.

[39] CMS Collaboration, "The CMS experiment at the CERN LHC", *JINST* **3** (2008) S08004, doi:10.1088/1748-0221/3/08/S08004.

[40] CMS Collaboration, "Development of the CMS detector for the CERN LHC Run 3", *JINST* **19** (2024) P05064, doi:10.1088/1748-0221/19/05/P05064, arXiv:2309.05466.

[41] CMS Collaboration, "Performance of the CMS Level-1 trigger in proton-proton collisions at $\sqrt{s} = 13$ TeV", *JINST* **15** (2020) P10017, doi:10.1088/1748-0221/15/10/P10017, arXiv:2006.10165.

[42] CMS Collaboration, "The CMS trigger system", *JINST* **12** (2017) P01020, doi:10.1088/1748-0221/12/01/P01020, arXiv:1609.02366.

[43] CMS Collaboration, "Particle-flow reconstruction and global event description with the CMS detector", *JINST* **12** (2017) P10003, doi:10.1088/1748-0221/12/10/P10003, arXiv:1706.04965.

[44] CMS Collaboration, "Technical proposal for the Phase-II upgrade of the Compact Muon Solenoid", CMS Technical Proposal CERN-LHCC-2015-010, CMS-TDR-15-02, 2015.

[45] CMS Collaboration, "Performance of the CMS muon detector and muon reconstruction with proton-proton collisions at $\sqrt{s} = 13$ TeV", *JINST* **13** (2018) P06015, doi:10.1088/1748-0221/13/06/P06015, arXiv:1804.04528.

[46] CMS Collaboration, "Electron and photon reconstruction and identification with the CMS experiment at the CERN LHC", *JINST* **16** (2021) P05014, doi:10.1088/1748-0221/16/05/P05014, arXiv:2012.06888.

[47] CMS Collaboration, "Pileup mitigation at CMS in 13 TeV data", *JINST* **15** (2020) P09018, doi:10.1088/1748-0221/15/09/p09018, arXiv:2003.00503.

[48] J. Alwall et al., "The automated computation of tree-level and next-to-leading order differential cross sections, and their matching to parton shower simulations", *JHEP* **07** (2014) 079, doi:10.1007/JHEP07(2014)079, arXiv:1405.0301.

[49] T. Sjöstrand et al., "An introduction to PYTHIA 8.2", *Comput. Phys. Commun.* **191** (2015) 159, doi:10.1016/j.cpc.2015.01.024, arXiv:1410.3012.

[50] CMS Collaboration, "Extraction and validation of a new set of CMS PYTHIA8 tunes from underlying-event measurements", *Eur. Phys. J. C* **80** (2020) 4, doi:10.1140/epjc/s10052-019-7499-4, arXiv:1903.12179.

[51] CMS Collaboration, "Event generator tunes obtained from underlying event and multiparton scattering measurements", *Eur. Phys. J. C* **76** (2016) 155, doi:10.1140/epjc/s10052-016-3988-x, arXiv:1512.00815.

[52] R. D. Ball et al., "A first unbiased global NLO determination of parton distributions and their uncertainties", *Nucl. Phys. B* **838** (2010) 136, doi:10.1016/j.nuclphysb.2010.05.008, arXiv:1002.4407.

[53] NNPDF Collaboration, "Parton distributions for the LHC Run II", *JHEP* **04** (2015) 040, doi:10.1007/JHEP04(2015)040, arXiv:1410.8849.

[54] NNPDF Collaboration, "Precision determination of the strong coupling constant within a global PDF analysis", *Eur. Phys. J. C* **78** (2018) 408, doi:10.1140/epjc/s10052-018-5897-7, arXiv:1802.03398.

[55] P. Nason, "A new method for combining NLO QCD with shower Monte Carlo algorithms", *JHEP* **11** (2004) 040, doi:10.1088/1126-6708/2004/11/040, arXiv:hep-ph/0409146.

[56] S. Frixione, P. Nason, and C. Oleari, "Matching NLO QCD computations with parton shower simulations: the POWHEG method", *JHEP* **11** (2007) 070, doi:10.1088/1126-6708/2007/11/070, arXiv:0709.2092.

[57] S. Alioli, P. Nason, C. Oleari, and E. Re, "A general framework for implementing NLO calculations in shower Monte Carlo programs: the POWHEG BOX", *JHEP* **06** (2010) 043, doi:10.1007/JHEP06(2010)043, arXiv:1002.2581.

[58] S. Frixione, P. Nason, and G. Ridolfi, "A positive-weight next-to-leading-order Monte Carlo for heavy flavour hadroproduction", *JHEP* **09** (2007) 126, doi:10.1088/1126-6708/2007/09/126, arXiv:0707.3088.

[59] CMS Collaboration, "Investigations of the impact of the parton shower tuning in Pythia8 in the modelling of $\mathrm{t\bar{t}}$ at $\sqrt{s} = 8$ and 13 TeV", CMS Physics Analysis Summary CMS-PAS-TOP-16-021, 2016.

[60] T. Melia, P. Nason, R. Rontsch, and G. Zanderighi, "W^+W^- , WZ and ZZ production in the POWHEG BOX", *JHEP* **11** (2011) 078, doi:10.1007/JHEP11(2011)078, arXiv:1107.5051.

[61] P. Nason and G. Zanderighi, "W^+W^- , WZ and ZZ production in the POWHEG-BOX-V2", *Eur. Phys. J. C* **74** (2014) 2702, doi:10.1140/epjc/s10052-013-2702-5, arXiv:1311.1365.

[62] L. Forthomme, "CepGen – A generic central exclusive processes event generator for hadron-hadron collisions", *Comput. Phys. Commun.* **271** (2022) 108225, doi:10.1016/j.cpc.2021.108225, arXiv:1808.06059.

[63] J. A. M. Vermaseren, "Two photon processes at very high-energies", *Nucl. Phys. B* **229** (1983) 347, doi:10.1016/0550-3213(83)90336-X.

[64] S. Baranov, O. Düenger, H. Shooshtari, and J. Vermaseren, "LPAIR: A generator for lepton pair production", in *Workshop on Physics at HERA*, p. 1478. 1991.

[65] T. Sjöstrand, S. Mrenna, and P. Z. Skands, "PYTHIA 6.4 physics and manual", *JHEP* **05** (2006) 026, doi:10.1088/1126-6708/2006/05/026, arXiv:hep-ph/0603175.

[66] A. Suri and D. R. Yennie, "The space-time phenomenology of photon absorbtion and inelastic electron scattering", *Annals Phys.* **72** (1972) 243, doi:10.1016/0003-4916(72)90242-4.

[67] J. M. Campbell, R. K. Ellis, and W. T. Giele, "A multi-threaded version of MCFM", *Eur. Phys. J. C* **75** (2015) 246, doi:10.1140/epjc/s10052-015-3461-2, arXiv:1503.06182.

[68] T. Gehrmann et al., "W^+W^- production at hadron colliders in next to next to leading order QCD", *Phys. Rev. Lett.* **113** (2014) 212001, doi:10.1103/PhysRevLett.113.212001, arXiv:1408.5243.

[69] M. Czakon and A. Mitov, "Top++: A program for the calculation of the top-pair cross-section at hadron colliders", *Comput. Phys. Commun.* **185** (2014) 2930, doi:10.1016/j.cpc.2014.06.021, arXiv:1112.5675.

[70] A. Crivellin and L. Schnell, "Complete Lagrangian and set of Feynman rules for scalar leptoquarks", *Comput. Phys. Commun.* **271** (2022) 108188, doi:10.1016/j.cpc.2021.108188, arXiv:2105.04844.

[71] GEANT4 Collaboration, "GEANT4 – a simulation toolkit", *Nucl. Instrum. Meth. A* **506** (2003) 250, doi:10.1016/S0168-9002(03)01368-8.

[72] CMS Collaboration, "Performance of the reconstruction and identification of high-momentum muons in proton-proton collisions at $\sqrt{s} = 13$ TeV", *JINST* **15** (2020) P02027, doi:10.1088/1748-0221/15/02/P02027, arXiv:1912.03516.

[73] CMS Collaboration, "Measurement of the differential Drell-Yan cross section in proton-proton collisions at $\sqrt{s} = 13$ TeV", *JHEP* **12** (2019) 059, doi:10.1007/JHEP12(2019)059, arXiv:1812.10529.

[74] CMS Collaboration, "Search for physics beyond the standard model in dilepton mass spectra in proton-proton collisions at $\sqrt{s} = 8$ TeV", *JHEP* **04** (2015) 025, doi:10.1007/JHEP04(2015)025, arXiv:1412.6302.

[75] Particle Data Group Collaboration, "Review of particle physics", *Phys. Rev. D* **110** (2024) 030001, doi:10.1103/PhysRevD.110.030001.

[76] CMS Collaboration, "Measurement of the top quark forward-backward production asymmetry and the anomalous chromoelectric and chromomagnetic moments in pp collisions at $\sqrt{s} = 13$ TeV", *JHEP* **06** (2020) 146, doi:10.1007/JHEP06(2020)146, arXiv:1912.09540.

[77] A. Manohar, P. Nason, G. P. Salam, and G. Zanderighi, "How bright is the proton? A precise determination of the photon parton distribution function", *Phys. Rev. Lett.* **117** (2016) 242002, doi:10.1103/PhysRevLett.117.242002, arXiv:1607.04266.

[78] A. V. Manohar, P. Nason, G. P. Salam, and G. Zanderighi, "The photon content of the proton", *JHEP* **12** (2017) 046, doi:10.1007/JHEP12(2017)046, arXiv:1708.01256.

[79] J. S. Conway, "Incorporating nuisance parameters in likelihoods for multisource spectra", in *PHYSTAT 2011*, p. 115. 2011. arXiv:1103.0354. doi:10.5170/CERN-2011-006.115.

[80] CMS Collaboration, "Precision luminosity measurement in proton-proton collisions at $\sqrt{s} = 13$ TeV in 2015 and 2016 at CMS", *Eur. Phys. J. C* **81** (2021) 800, doi:10.1140/epjc/s10052-021-09538-2, arXiv:2104.01927.

[81] CMS Collaboration, "CMS luminosity measurement for the 2017 data-taking period at $\sqrt{s}$ = 13 TeV", CMS Physics Analysis Summary CMS-PAS-LUM-17-004, 2018.

[82] CMS Collaboration, "CMS luminosity measurement for the 2018 data-taking period at $\sqrt{s}$ = 13 TeV", CMS Physics Analysis Summary CMS-PAS-LUM-18-002, 2019.

[83] CMS Collaboration, "The CMS statistical analysis and combination tool: COMBINE", *Comput. Softw. Big Sci.* **8** (2024) 19, doi:10.1007/s41781-024-00121-4, arXiv:2404.06614.

[84] G. J. Feldman and R. D. Cousins, "Unified approach to the classical statistical analysis of small signals", *Phys. Rev. D* **57** (1998) 3873, doi:10.1103/PhysRevD.57.3873, arXiv:physics/9711021.

[85] T. Junk, "Confidence level computation for combining searches with small statistics", *Nucl. Instrum. Meth. A* **434** (1999) 435, doi:10.1016/S0168-9002(99)00498-2, arXiv:hep-ex/9902006.

[86] A. L. Read, "Presentation of search results: The CL_s technique", *J. Phys. G* **28** (2002) 2693, doi:10.1088/0954-3899/28/10/313.

[87] G. Cowan, K. Cranmer, E. Gross, and O. Vitells, "Asymptotic formulae for likelihood-based tests of new physics", *Eur. Phys. J. C* **71** (2011) 1554, doi:10.1140/epjc/s10052-011-1554-0, arXiv:1007.1727. [Erratum: doi:10.1140/epjc/s10052-011-1554-0].

A The CMS Collaboration

Yerevan Physics Institute, Yerevan, Armenia
A. Hayrapetyan, A. Tumasyan[1]

Institut für Hochenergiephysik, Vienna, Austria
W. Adam, J.W. Andrejkovic, L. Benato, T. Bergauer, S. Chatterjee, K. Damanakis, M. Dragicevic, P.S. Hussain, M. Jeitler[2], N. Krammer, A. Li, D. Liko, I. Mikulec, J. Schieck[2], R. Schöfbeck[2], D. Schwarz, M. Sonawane, W. Waltenberger, C.-E. Wulz[2]

Universiteit Antwerpen, Antwerpen, Belgium
T. Janssen, T. Van Laer, P. Van Mechelen

Vrije Universiteit Brussel, Brussel, Belgium
N. Breugelmans, J. D'Hondt, S. Dansana, A. De Moor, M. Delcourt, F. Heyen, S. Lowette, I. Makarenko, D. Müller, S. Tavernier, M. Tytgat[3], G.P. Van Onsem, S. Van Putte, D. Vannerom

Université Libre de Bruxelles, Bruxelles, Belgium
B. Bilin, B. Clerbaux, A.K. Das, I. De Bruyn, G. De Lentdecker, H. Evard, L. Favart, P. Gianneios, J. Jaramillo, A. Khalilzadeh, F.A. Khan, K. Lee, A. Malara, M.A. Shahzad, L. Thomas, M. Vanden Bemden, C. Vander Velde, P. Vanlaer

Ghent University, Ghent, Belgium
M. De Coen, D. Dobur, G. Gokbulut, Y. Hong, J. Knolle, L. Lambrecht, D. Marckx, K. Mota Amarilo, K. Skovpen, N. Van Den Bossche, J. van der Linden, L. Wezenbeek

Université Catholique de Louvain, Louvain-la-Neuve, Belgium
A. Benecke, A. Bethani, G. Bruno, C. Caputo, J. De Favereau De Jeneret, C. Delaere, I.S. Donertas, A. Giammanco, A.O. Guzel, Sa. Jain, V. Lemaitre, J. Lidrych, P. Mastrapasqua, T.T. Tran, S. Turkcapar

Centro Brasileiro de Pesquisas Fisicas, Rio de Janeiro, Brazil
G.A. Alves, E. Coelho, G. Correia Silva, C. Hensel, T. Menezes De Oliveira, C. Mora Herrera[4], P. Rebello Teles, M. Soeiro, E.J. Tonelli Manganote[5], A. Vilela Pereira[4]

Universidade do Estado do Rio de Janeiro, Rio de Janeiro, Brazil
W.L. Aldá Júnior, M. Barroso Ferreira Filho, H. Brandao Malbouisson, W. Carvalho, J. Chinellato[6], E.M. Da Costa, G.G. Da Silveira[7], D. De Jesus Damiao, S. Fonseca De Souza, R. Gomes De Souza, T. Laux Kuhn[7], M. Macedo, J. Martins, L. Mundim, H. Nogima, J.P. Pinheiro, A. Santoro, A. Sznajder, M. Thiel

Universidade Estadual Paulista, Universidade Federal do ABC, São Paulo, Brazil
C.A. Bernardes[7], L. Calligaris, T.R. Fernandez Perez Tomei, E.M. Gregores, I. Maietto Silverio, P.G. Mercadante, S.F. Novaes, B. Orzari, Sandra S. Padula

Institute for Nuclear Research and Nuclear Energy, Bulgarian Academy of Sciences, Sofia, Bulgaria
A. Aleksandrov, G. Antchev, R. Hadjiiska, P. Iaydjiev, M. Misheva, M. Shopova, G. Sultanov

University of Sofia, Sofia, Bulgaria
A. Dimitrov, L. Litov, B. Pavlov, P. Petkov, A. Petrov, E. Shumka

Instituto De Alta Investigación, Universidad de Tarapacá, Casilla 7 D, Arica, Chile
S. Keshri, D. Laroze, S. Thakur

Beihang University, Beijing, China
T. Cheng, T. Javaid, L. Yuan

Department of Physics, Tsinghua University, Beijing, China
Z. Hu, Z. Liang, J. Liu

Institute of High Energy Physics, Beijing, China
G.M. Chen[8], H.S. Chen[8], M. Chen[8], F. Iemmi, C.H. Jiang, A. Kapoor[9], H. Liao, Z.-A. Liu[10], R. Sharma[11], J.N. Song[10], J. Tao, C. Wang[8], J. Wang, Z. Wang[8], H. Zhang, J. Zhao

State Key Laboratory of Nuclear Physics and Technology, Peking University, Beijing, China
A. Agapitos, Y. Ban, A. Carvalho Antunes De Oliveira, S. Deng, B. Guo, C. Jiang, A. Levin, C. Li, Q. Li, Y. Mao, S. Qian, S.J. Qian, X. Qin, X. Sun, D. Wang, H. Yang, L. Zhang, Y. Zhao, C. Zhou

Guangdong Provincial Key Laboratory of Nuclear Science and Guangdong-Hong Kong Joint Laboratory of Quantum Matter, South China Normal University, Guangzhou, China
S. Yang

Sun Yat-Sen University, Guangzhou, China
Z. You

University of Science and Technology of China, Hefei, China
K. Jaffel, N. Lu

Nanjing Normal University, Nanjing, China
G. Bauer[12], B. Li[13], K. Yi[14], J. Zhang

Institute of Modern Physics and Key Laboratory of Nuclear Physics and Ion-beam Application (MOE) - Fudan University, Shanghai, China
Y. Li

Zhejiang University, Hangzhou, Zhejiang, China
Z. Lin, C. Lu, M. Xiao

Universidad de Los Andes, Bogota, Colombia
C. Avila, D.A. Barbosa Trujillo, A. Cabrera, C. Florez, J. Fraga, J.A. Reyes Vega

Universidad de Antioquia, Medellin, Colombia
C. Rendón, M. Rodriguez, A.A. Ruales Barbosa, J.D. Ruiz Alvarez

University of Split, Faculty of Electrical Engineering, Mechanical Engineering and Naval Architecture, Split, Croatia
D. Giljanovic, N. Godinovic, D. Lelas, A. Sculac

University of Split, Faculty of Science, Split, Croatia
M. Kovac, A. Petkovic, T. Sculac

Institute Rudjer Boskovic, Zagreb, Croatia
P. Bargassa, V. Brigljevic, B.K. Chitroda, D. Ferencek, K. Jakovcic, A. Starodumov[15],

T. Susa

University of Cyprus, Nicosia, Cyprus
A. Attikis, K. Christoforou, A. Hadjiagapiou, C. Leonidou, J. Mousa, C. Nicolaou, L. Paizanos, F. Ptochos, P.A. Razis, H. Rykaczewski, H. Saka, A. Stepennov

Charles University, Prague, Czech Republic
M. Finger, M. Finger Jr., A. Kveton

Escuela Politecnica Nacional, Quito, Ecuador
E. Ayala

Universidad San Francisco de Quito, Quito, Ecuador
E. Carrera Jarrin

Academy of Scientific Research and Technology of the Arab Republic of Egypt, Egyptian Network of High Energy Physics, Cairo, Egypt
B. El-mahdy, S. Khalil[16], E. Salama[17,18]

Center for High Energy Physics (CHEP-FU), Fayoum University, El-Fayoum, Egypt
M. Abdullah Al-Mashad, M.A. Mahmoud

National Institute of Chemical Physics and Biophysics, Tallinn, Estonia
K. Ehataht, M. Kadastik, T. Lange, C. Nielsen, J. Pata, M. Raidal, L. Tani, C. Veelken

Department of Physics, University of Helsinki, Helsinki, Finland
H. Kirschenmann, K. Osterberg, M. Voutilainen

Helsinki Institute of Physics, Helsinki, Finland
S. Bharthuar, N. Bin Norjoharuddeen, E. Brücken, F. Garcia, P. Inkaew, K.T.S. Kallonen, T. Lampén, K. Lassila-Perini, S. Lehti, T. Lindén, M. Myllymäki, M.m. Rantanen, H. Siikonen, J. Tuominiemi

Lappeenranta-Lahti University of Technology, Lappeenranta, Finland
P. Luukka, H. Petrow

IRFU, CEA, Université Paris-Saclay, Gif-sur-Yvette, France
M. Besancon, F. Couderc, M. Dejardin, D. Denegri, J.L. Faure, F. Ferri, S. Ganjour, P. Gras, G. Hamel de Monchenault, M. Kumar, V. Lohezic, J. Malcles, F. Orlandi, L. Portales, A. Rosowsky, M.Ö. Sahin, A. Savoy-Navarro[19], P. Simkina, M. Titov, M. Tornago

Laboratoire Leprince-Ringuet, CNRS/IN2P3, Ecole Polytechnique, Institut Polytechnique de Paris, Palaiseau, France
F. Beaudette, G. Boldrini, P. Busson, A. Cappati, C. Charlot, M. Chiusi, T.D. Cuisset, F. Damas, O. Davignon, A. De Wit, I.T. Ehle, B.A. Fontana Santos Alves, S. Ghosh, A. Gilbert, R. Granier de Cassagnac, A. Hakimi, B. Harikrishnan, L. Kalipoliti, G. Liu, M. Nguyen, C. Ochando, R. Salerno, J.B. Sauvan, Y. Sirois, L. Urda Gómez, E. Vernazza, A. Zabi, A. Zghiche

Université de Strasbourg, CNRS, IPHC UMR 7178, Strasbourg, France
J.-L. Agram[20], J. Andrea, D. Apparu, D. Bloch, J.-M. Brom, E.C. Chabert, C. Collard, S. Falke, U. Goerlach, R. Haeberle, A.-C. Le Bihan, M. Meena, O. Poncet, G. Saha, M.A. Sessini, P. Van Hove, P. Vaucelle

Centre de Calcul de l'Institut National de Physique Nucleaire et de Physique des Particules, CNRS/IN2P3, Villeurbanne, France
A. Di Florio

Institut de Physique des 2 Infinis de Lyon (IP2I), Villeurbanne, France
D. Amram, S. Beauceron, B. Blancon, G. Boudoul, N. Chanon, D. Contardo, P. Depasse, C. Dozen[21], H. El Mamouni, J. Fay, S. Gascon, M. Gouzevitch, C. Greenberg, G. Grenier, B. Ille, E. Jourd'huy, M. Lethuillier, L. Mirabito, S. Perries, A. Purohit, M. Vander Donckt, P. Verdier, J. Xiao

Georgian Technical University, Tbilisi, Georgia
D. Chokheli, I. Lomidze, Z. Tsamalaidze[22]

RWTH Aachen University, I. Physikalisches Institut, Aachen, Germany
V. Botta, S. Consuegra Rodríguez, L. Feld, K. Klein, M. Lipinski, D. Meuser, A. Pauls, D. Pérez Adán, N. Röwert, M. Teroerde

RWTH Aachen University, III. Physikalisches Institut A, Aachen, Germany
S. Diekmann, A. Dodonova, N. Eich, D. Eliseev, F. Engelke, J. Erdmann, M. Erdmann, P. Fackeldey, B. Fischer, T. Hebbeker, K. Hoepfner, F. Ivone, A. Jung, M.y. Lee, F. Mausolf, M. Merschmeyer, A. Meyer, S. Mukherjee, D. Noll, F. Nowotny, A. Pozdnyakov, Y. Rath, W. Redjeb, F. Rehm, H. Reithler, V. Sarkisovi, A. Schmidt, C. Seth, A. Sharma, J.L. Spah, A. Stein, F. Torres Da Silva De Araujo[23], S. Wiedenbeck, S. Zaleski

RWTH Aachen University, III. Physikalisches Institut B, Aachen, Germany
C. Dziwok, G. Flügge, T. Kress, A. Nowack, O. Pooth, A. Stahl, T. Ziemons, A. Zotz

Deutsches Elektronen-Synchrotron, Hamburg, Germany
H. Aarup Petersen, M. Aldaya Martin, J. Alimena, S. Amoroso, Y. An, J. Bach, S. Baxter, M. Bayatmakou, H. Becerril Gonzalez, O. Behnke, A. Belvedere, F. Blekman[24], K. Borras[25], A. Campbell, A. Cardini, C. Cheng, F. Colombina, G. Eckerlin, D. Eckstein, L.I. Estevez Banos, E. Gallo[24], A. Geiser, V. Guglielmi, M. Guthoff, A. Hinzmann, L. Jeppe, B. Kaech, M. Kasemann, C. Kleinwort, R. Kogler, M. Komm, D. Krücker, W. Lange, D. Leyva Pernia, K. Lipka[26], W. Lohmann[27], F. Lorkowski, R. Mankel, I.-A. Melzer-Pellmann, M. Mendizabal Morentin, A.B. Meyer, G. Milella, K. Moral Figueroa, A. Mussgiller, L.P. Nair, J. Niedziela, A. Nürnberg, Y. Otarid, J. Park, E. Ranken, A. Raspereza, D. Rastorguev, J. Rübenach, L. Rygaard, A. Saggio, M. Scham[28,25], S. Schnake[25], P. Schütze, C. Schwanenberger[24], D. Selivanova, K. Sharko, M. Shchedrolosiev, D. Stafford, F. Vazzoler, A. Ventura Barroso, R. Walsh, D. Wang, Q. Wang, K. Wichmann, L. Wiens[25], C. Wissing, Y. Yang, A. Zimermmane Castro Santos

University of Hamburg, Hamburg, Germany
A. Albrecht, S. Albrecht, M. Antonello, S. Bein, S. Bollweg, M. Bonanomi, P. Connor, K. El Morabit, Y. Fischer, E. Garutti, A. Grohsjean, J. Haller, D. Hundhausen, H.R. Jabusch, G. Kasieczka, P. Keicher, R. Klanner, W. Korcari, T. Kramer, C.c. Kuo, V. Kutzner, F. Labe, J. Lange, A. Lobanov, C. Matthies, L. Moureaux, M. Mrowietz, A. Nigamova, Y. Nissan, A. Paasch, K.J. Pena Rodriguez, T. Quadfasel, B. Raciti, M. Rieger, D. Savoiu, J. Schindler, P. Schleper, M. Schröder, J. Schwandt, M. Sommerhalder, H. Stadie, G. Steinbrück, A. Tews, B. Wiederspan, M. Wolf

Karlsruher Institut fuer Technologie, Karlsruhe, Germany
S. Brommer, E. Butz, T. Chwalek, A. Dierlamm, A. Droll, U. Elicabuk, N. Faltermann, M. Giffels, A. Gottmann, F. Hartmann[29], R. Hofsaess, M. Horzela, U. Husemann, J. Kieseler, M. Klute, O. Lavoryk, J.M. Lawhorn, M. Link, A. Lintuluoto, S. Maier, S. Mitra, M. Mormile, Th. Müller, M. Neukum, M. Oh, E. Pfeffer, M. Presilla, G. Quast, K. Rabbertz, B. Regnery, N. Shadskiy, I. Shvetsov, H.J. Simonis, L. Sowa, L. Stockmeier, K. Tauqeer, M. Toms, B. Topko, N. Trevisani, R.F. Von Cube, M. Wassmer, S. Wieland, F. Wittig, R. Wolf, X. Zuo

Institute of Nuclear and Particle Physics (INPP), NCSR Demokritos, Aghia Paraskevi, Greece
G. Anagnostou, G. Daskalakis, A. Kyriakis, A. Papadopoulos[29], A. Stakia

National and Kapodistrian University of Athens, Athens, Greece
G. Melachroinos, Z. Painesis, I. Paraskevas, N. Saoulidou, K. Theofilatos, E. Tziaferi, K. Vellidis, I. Zisopoulos

National Technical University of Athens, Athens, Greece
G. Bakas, T. Chatzistavrou, G. Karapostoli, K. Kousouris, I. Papakrivopoulos, E. Siamarkou, G. Tsipolitis, A. Zacharopoulou

University of Ioánnina, Ioánnina, Greece
I. Bestintzanos, I. Evangelou, C. Foudas, C. Kamtsikis, P. Katsoulis, P. Kokkas, P.G. Kosmoglou Kioseoglou, N. Manthos, I. Papadopoulos, J. Strologas

HUN-REN Wigner Research Centre for Physics, Budapest, Hungary
C. Hajdu, D. Horvath[30,31], K. Márton, A.J. Rádl[32], F. Sikler, V. Veszpremi

MTA-ELTE Lendület CMS Particle and Nuclear Physics Group, Eötvös Loránd University, Budapest, Hungary
M. Csanád, K. Farkas, A. Fehérkuti[33], M.M.A. Gadallah[34], Á. Kadlecsik, P. Major, G. Pásztor, G.I. Veres

Faculty of Informatics, University of Debrecen, Debrecen, Hungary
B. Ujvari, G. Zilizi

HUN-REN ATOMKI - Institute of Nuclear Research, Debrecen, Hungary
G. Bencze, S. Czellar, J. Molnar, Z. Szillasi

Karoly Robert Campus, MATE Institute of Technology, Gyongyos, Hungary
T. Csorgo[33], F. Nemes[33], T. Novak

Panjab University, Chandigarh, India
S. Bansal, S.B. Beri, V. Bhatnagar, G. Chaudhary, S. Chauhan, N. Dhingra[35], A. Kaur, A. Kaur, H. Kaur, M. Kaur, S. Kumar, T. Sheokand, J.B. Singh, A. Singla

University of Delhi, Delhi, India
A. Ahmed, A. Bhardwaj, A. Chhetri, B.C. Choudhary, A. Kumar, A. Kumar, M. Naimuddin, K. Ranjan, M.K. Saini, S. Saumya

Saha Institute of Nuclear Physics, HBNI, Kolkata, India
S. Baradia, S. Barman[36], S. Bhattacharya, S. Das Gupta, S. Dutta, S. Dutta, S. Sarkar

Indian Institute of Technology Madras, Madras, India
M.M. Ameen, P.K. Behera, S.C. Behera, S. Chatterjee, G. Dash, P. Jana,

P. Kalbhor, S. Kamble, J.R. Komaragiri[37], D. Kumar[37], T. Mishra, B. Parida[38], P.R. Pujahari, N.R. Saha, A. Sharma, A.K. Sikdar, R.K. Singh, P. Verma, S. Verma, A. Vijay

Tata Institute of Fundamental Research-A, Mumbai, India
S. Dugad, G.B. Mohanty, M. Shelake, P. Suryadevara

Tata Institute of Fundamental Research-B, Mumbai, India
A. Bala, S. Banerjee, R.M. Chatterjee, M. Guchait, Sh. Jain, A. Jaiswal, S. Kumar, G. Majumder, K. Mazumdar, S. Parolia, A. Thachayath

National Institute of Science Education and Research, An OCC of Homi Bhabha National Institute, Bhubaneswar, Odisha, India
S. Bahinipati[39], C. Kar, D. Maity[40], P. Mal, K. Naskar[40], A. Nayak[40], S. Nayak, K. Pal, P. Sadangi, S.K. Swain, S. Varghese[40], D. Vats[40]

Indian Institute of Science Education and Research (IISER), Pune, India
S. Acharya[41], A. Alpana, S. Dube, B. Gomber[41], P. Hazarika, B. Kansal, A. Laha, B. Sahu[41], S. Sharma, K.Y. Vaish

Isfahan University of Technology, Isfahan, Iran
H. Bakhshiansohi[42], A. Jafari[43], M. Zeinali[44]

Institute for Research in Fundamental Sciences (IPM), Tehran, Iran
S. Bashiri, S. Chenarani[45], S.M. Etesami, Y. Hosseini, M. Khakzad, E. Khazaie, M. Mohammadi Najafabadi, S. Tizchang[46]

University College Dublin, Dublin, Ireland
M. Felcini, M. Grunewald

INFN Sezione di Bari[a], Università di Bari[b], Politecnico di Bari[c], Bari, Italy
M. Abbrescia[a,b], A. Colaleo[a,b], D. Creanza[a,c], B. D'Anzi[a,b], N. De Filippis[a,c], M. De Palma[a,b], W. Elmetenawee[a,b,47], N. Ferrara[a,b], L. Fiore[a], G. Iaselli[a,c], L. Longo[a], M. Louka[a,b], G. Maggi[a,c], M. Maggi[a], I. Margjeka[a], V. Mastrapasqua[a,b], S. My[a,b], S. Nuzzo[a,b], A. Pellecchia[a,b], A. Pompili[a,b], G. Pugliese[a,c], R. Radogna[a,b], D. Ramos[a], A. Ranieri[a], L. Silvestris[a], F.M. Simone[a,c], Ü. Sözbilir[a], A. Stamerra[a,b], D. Troiano[a,b], R. Venditti[a,b], P. Verwilligen[a], A. Zaza[a,b]

INFN Sezione di Bologna[a], Università di Bologna[b], Bologna, Italy
G. Abbiendi[a], C. Battilana[a,b], D. Bonacorsi[a,b], P. Capiluppi[a,b], A. Castro[†a,b], F.R. Cavallo[a], M. Cuffiani[a,b], G.M. Dallavalle[a], T. Diotalevi[a,b], F. Fabbri[a], A. Fanfani[a,b], D. Fasanella[a], P. Giacomelli[a], L. Giommi[a,b], C. Grandi[a], L. Guiducci[a,b], S. Lo Meo[a,48], M. Lorusso[a,b], L. Lunerti[a], S. Marcellini[a], G. Masetti[a], F.L. Navarria[a,b], G. Paggi[a,b], A. Perrotta[a], F. Primavera[a,b], A.M. Rossi[a,b], S. Rossi Tisbeni[a,b], T. Rovelli[a,b], G.P. Siroli[a,b]

INFN Sezione di Catania[a], Università di Catania[b], Catania, Italy
S. Costa[a,b,49], A. Di Mattia[a], A. Lapertosa[a], R. Potenza[a,b], A. Tricomi[a,b,49], C. Tuve[a,b]

INFN Sezione di Firenze[a], Università di Firenze[b], Firenze, Italy
P. Assiouras[a], G. Barbagli[a], G. Bardelli[a,b], B. Camaiani[a,b], A. Cassese[a], R. Ceccarelli[a], V. Ciulli[a,b], C. Civinini[a], R. D'Alessandro[a,b], E. Focardi[a,b], T. Kello[a], G. Latino[a,b], P. Lenzi[a,b], M. Lizzo[a], M. Meschini[a], S. Paoletti[a],

A. Papanastassiou[a,b], G. Sguazzoni[a], L. Viliani[a]

INFN Laboratori Nazionali di Frascati, Frascati, Italy
L. Benussi, S. Bianco, S. Meola[50], D. Piccolo

INFN Sezione di Genova[a], Università di Genova[b], Genova, Italy
M. Alves Gallo Pereira[a], F. Ferro[a], E. Robutti[a], S. Tosi[a,b]

INFN Sezione di Milano-Bicocca[a], Università di Milano-Bicocca[b], Milano, Italy
A. Benaglia[a], F. Brivio[a], F. Cetorelli[a,b], F. De Guio[a,b], M.E. Dinardo[a,b], P. Dini[a], S. Gennai[a], R. Gerosa[a,b], A. Ghezzi[a,b], P. Govoni[a,b], L. Guzzi[a], M.T. Lucchini[a,b], M. Malberti[a], S. Malvezzi[a], A. Massironi[a], D. Menasce[a], L. Moroni[a], M. Paganoni[a,b], S. Palluotto[a,b], D. Pedrini[a], A. Perego[a,b], B.S. Pinolini[a], G. Pizzati[a,b], S. Ragazzi[a,b], T. Tabarelli de Fatis[a,b]

INFN Sezione di Napoli[a], Università di Napoli 'Federico II'[b], Napoli, Italy; Università della Basilicata[c], Potenza, Italy; Scuola Superiore Meridionale (SSM)[d], Napoli, Italy
S. Buontempo[a], A. Cagnotta[a,b], F. Carnevali[a,b], N. Cavallo[a,c], F. Fabozzi[a,c], A.O.M. Iorio[a,b], L. Lista[a,b,51], P. Paolucci[a,29], B. Rossi[a]

INFN Sezione di Padova[a], Università di Padova[b], Padova, Italy; Università di Trento[c], Trento, Italy
R. Ardino[a], P. Azzi[a], N. Bacchetta[a,52], D. Bisello[a,b], P. Bortignon[a], G. Bortolato[a,b], A. Bragagnolo[a,b], A.C.M. Bulla[a], R. Carlin[a,b], T. Dorigo[a,53], F. Gasparini[a,b], U. Gasparini[a,b], S. Giorgetti[a], E. Lusiani[a], M. Margoni[a,b], A.T. Meneguzzo[a,b], M. Migliorini[a,b], M. Passaseo[a], J. Pazzini[a,b], P. Ronchese[a,b], R. Rossin[a,b], M. Sgaravatto[a], F. Simonetto[a,b], M. Tosi[a,b], A. Triossi[a,b], S. Ventura[a], M. Zanetti[a,b], P. Zotto[a,b], A. Zucchetta[a,b]

INFN Sezione di Pavia[a], Università di Pavia[b], Pavia, Italy
A. Braghieri[a], S. Calzaferri[a], D. Fiorina[a], P. Montagna[a,b], V. Re[a], C. Riccardi[a,b], P. Salvini[a], I. Vai[a,b], P. Vitulo[a,b]

INFN Sezione di Perugia[a], Università di Perugia[b], Perugia, Italy
S. Ajmal[a,b], M.E. Ascioti[a,b], G.M. Bilei[a], C. Carrivale[a,b], D. Ciangottini[a,b], L. Fanò[a,b], M. Magherini[a,b], V. Mariani[a,b], M. Menichelli[a], F. Moscatelli[a,54], A. Rossi[a,b], A. Santocchia[a,b], D. Spiga[a], T. Tedeschi[a,b]

INFN Sezione di Pisa[a], Università di Pisa[b], Scuola Normale Superiore di Pisa[c], Pisa, Italy; Università di Siena[d], Siena, Italy
C. Aimè[a], C.A. Alexe[a,c], P. Asenov[a,b], P. Azzurri[a], G. Bagliesi[a], R. Bhattacharya[a], L. Bianchini[a,b], T. Boccali[a], E. Bossini[a], D. Bruschini[a,c], R. Castaldi[a], M.A. Ciocci[a,b], M. Cipriani[a,b], V. D'Amante[a,d], R. Dell'Orso[a], S. Donato[a], A. Giassi[a], F. Ligabue[a,c], A.C. Marini[a,b], D. Matos Figueiredo[a], A. Messineo[a,b], S. Mishra[a], V.K. Muraleedharan Nair Bindhu[a,b,40], M. Musich[a,b], S. Nandan[a,b], F. Palla[a], A. Rizzi[a,b], G. Rolandi[a,c], S. Roy Chowdhury[a], T. Sarkar[a], A. Scribano[a], P. Spagnolo[a], R. Tenchini[a], G. Tonelli[a,b], N. Turini[a,d], F. Vaselli[a,c], A. Venturi[a], P.G. Verdini[a]

INFN Sezione di Roma[a], Sapienza Università di Roma[b], Roma, Italy
C. Baldenegro Barrera[a,b], P. Barria[a], C. Basile[a,b], F. Cavallari[a], L. Cunqueiro Mendez[a,b], D. Del Re[a,b], E. Di Marco[a,b], M. Diemoz[a], F. Errico[a,b], R. Gargiulo[a,b], E. Longo[a,b], L. Martikainen[a,b], J. Mijuskovic[a,b], G. Organtini[a,b], F. Pandolfi[a], R. Paramatti[a,b], C. Quaranta[a,b], S. Rahatlou[a,b], C. Rovelli[a],

F. Santanastasio[a,b], L. Soffi[a], V. Vladimirov[a,b]

INFN Sezione di Torino[a], Università di Torino[b], Torino, Italy; Università del Piemonte Orientale[c], Novara, Italy
N. Amapane[a,b], R. Arcidiacono[a,c], S. Argiro[a,b], M. Arneodo[a,c], N. Bartosik[a], R. Bellan[a,b], A. Bellora[a,b], C. Biino[a], C. Borca[a,b], N. Cartiglia[a], M. Costa[a,b], R. Covarelli[a,b], N. Demaria[a], L. Finco[a], M. Grippo[a,b], B. Kiani[a,b], F. Legger[a], F. Luongo[a,b], C. Mariotti[a], L. Markovic[a,b], S. Maselli[a], A. Mecca[a,b], L. Menzio[a,b], P. Meridiani[a], E. Migliore[a,b], M. Monteno[a], R. Mulargia[a], M.M. Obertino[a,b], G. Ortona[a], L. Pacher[a,b], N. Pastrone[a], M. Pelliccioni[a], M. Ruspa[a,c], F. Siviero[a,b], V. Sola[a,b], A. Solano[a,b], A. Staiano[a], C. Tarricone[a,b], D. Trocino[a], G. Umoret[a,b], R. White[a,b]

INFN Sezione di Trieste[a], Università di Trieste[b], Trieste, Italy
J. Babbar[a,b], S. Belforte[a], V. Candelise[a,b], M. Casarsa[a], F. Cossutti[a], K. De Leo[a], G. Della Ricca[a,b]

Kyungpook National University, Daegu, Korea
S. Dogra, J. Hong, B. Kim, J. Kim, D. Lee, H. Lee, S.W. Lee, C.S. Moon, Y.D. Oh, M.S. Ryu, S. Sekmen, B. Tae, Y.C. Yang

Department of Mathematics and Physics - GWNU, Gangneung, Korea
M.S. Kim

Chonnam National University, Institute for Universe and Elementary Particles, Kwangju, Korea
G. Bak, P. Gwak, H. Kim, D.H. Moon

Hanyang University, Seoul, Korea
E. Asilar, J. Choi[55], D. Kim, T.J. Kim, J.A. Merlin, Y. Ryou

Korea University, Seoul, Korea
S. Choi, S. Han, B. Hong, K. Lee, K.S. Lee, S. Lee, J. Yoo

Kyung Hee University, Department of Physics, Seoul, Korea
J. Goh, S. Yang

Sejong University, Seoul, Korea
H. S. Kim, Y. Kim, S. Lee

Seoul National University, Seoul, Korea
J. Almond, J.H. Bhyun, J. Choi, J. Choi, W. Jun, J. Kim, Y.W. Kim, S. Ko, H. Kwon, H. Lee, J. Lee, J. Lee, B.H. Oh, S.B. Oh, H. Seo, U.K. Yang, I. Yoon

University of Seoul, Seoul, Korea
W. Jang, D.Y. Kang, Y. Kang, S. Kim, B. Ko, J.S.H. Lee, Y. Lee, I.C. Park, Y. Roh, I.J. Watson

Yonsei University, Department of Physics, Seoul, Korea
S. Ha, K. Hwang, H.D. Yoo

Sungkyunkwan University, Suwon, Korea
M. Choi, M.R. Kim, H. Lee, Y. Lee, I. Yu

College of Engineering and Technology, American University of the Middle East (AUM), Dasman, Kuwait

T. Beyrouthy, Y. Gharbia

Kuwait University - College of Science - Department of Physics, Safat, Kuwait
F. Alazemi

Riga Technical University, Riga, Latvia
K. Dreimanis, A. Gaile, C. Munoz Diaz, D. Osite, G. Pikurs, A. Potrebko, M. Seidel, D. Sidiropoulos Kontos

University of Latvia (LU), Riga, Latvia
N.R. Strautnieks

Vilnius University, Vilnius, Lithuania
M. Ambrozas, A. Juodagalvis, A. Rinkevicius, G. Tamulaitis

National Centre for Particle Physics, Universiti Malaya, Kuala Lumpur, Malaysia
I. Yusuff[56], Z. Zolkapli

Universidad de Sonora (UNISON), Hermosillo, Mexico
J.F. Benitez, A. Castaneda Hernandez, H.A. Encinas Acosta, L.G. Gallegos Maríñez, M. León Coello, J.A. Murillo Quijada, A. Sehrawat, L. Valencia Palomo

Centro de Investigacion y de Estudios Avanzados del IPN, Mexico City, Mexico
G. Ayala, H. Castilla-Valdez, H. Crotte Ledesma, E. De La Cruz-Burelo, I. Heredia-De La Cruz[57], R. Lopez-Fernandez, J. Mejia Guisao, C.A. Mondragon Herrera, A. Sánchez Hernández

Universidad Iberoamericana, Mexico City, Mexico
C. Oropeza Barrera, D.L. Ramirez Guadarrama, M. Ramírez García

Benemerita Universidad Autonoma de Puebla, Puebla, Mexico
I. Bautista, F.E. Neri Huerta, I. Pedraza, H.A. Salazar Ibarguen, C. Uribe Estrada

University of Montenegro, Podgorica, Montenegro
I. Bubanja, N. Raicevic

University of Canterbury, Christchurch, New Zealand
P.H. Butler

National Centre for Physics, Quaid-I-Azam University, Islamabad, Pakistan
A. Ahmad, M.I. Asghar, A. Awais, M.I.M. Awan, H.R. Hoorani, W.A. Khan

AGH University of Krakow, Krakow, Poland
V. Avati, L. Grzanka, M. Malawski

National Centre for Nuclear Research, Swierk, Poland
H. Bialkowska, M. Bluj, M. Górski, M. Kazana, M. Szleper, P. Zalewski

Institute of Experimental Physics, Faculty of Physics, University of Warsaw, Warsaw, Poland
K. Bunkowski, K. Doroba, A. Kalinowski, M. Konecki, J. Krolikowski, A. Muhammad

Warsaw University of Technology, Warsaw, Poland
P. Fokow, K. Pozniak, W. Zabolotny

Laboratório de Instrumentação e Física Experimental de Partículas, Lisboa, Portugal
M. Araujo, D. Bastos, C. Beirão Da Cruz E Silva, A. Boletti, M. Bozzo, T. Camporesi, G. Da Molin, P. Faccioli, M. Gallinaro, J. Hollar, N. Leonardo,

G.B. Marozzo, A. Petrilli, M. Pisano, J. Seixas, J. Varela, J.W. Wulff

Faculty of Physics, University of Belgrade, Belgrade, Serbia
P. Adzic, P. Milenovic

VINCA Institute of Nuclear Sciences, University of Belgrade, Belgrade, Serbia
D. Devetak, M. Dordevic, J. Milosevic, L. Nadderd, V. Rekovic

Centro de Investigaciones Energéticas Medioambientales y Tecnológicas (CIEMAT), Madrid, Spain
J. Alcaraz Maestre, Cristina F. Bedoya, J.A. Brochero Cifuentes, Oliver M. Carretero, M. Cepeda, M. Cerrada, N. Colino, B. De La Cruz, A. Delgado Peris, A. Escalante Del Valle, D. Fernández Del Val, J.P. Fernández Ramos, J. Flix, M.C. Fouz, O. Gonzalez Lopez, S. Goy Lopez, J.M. Hernandez, M.I. Josa, J. Llorente Merino, C. Martin Perez, E. Martin Viscasillas, D. Moran, C. M. Morcillo Perez, Á. Navarro Tobar, C. Perez Dengra, A. Pérez-Calero Yzquierdo, J. Puerta Pelayo, I. Redondo, S. Sánchez Navas, J. Sastre, J. Vazquez Escobar

Universidad Autónoma de Madrid, Madrid, Spain
J.F. de Trocóniz

Universidad de Oviedo, Instituto Universitario de Ciencias y Tecnologías Espaciales de Asturias (ICTEA), Oviedo, Spain
B. Alvarez Gonzalez, J. Cuevas, J. Fernandez Menendez, S. Folgueras, I. Gonzalez Caballero, P. Leguina, E. Palencia Cortezon, J. Prado Pico, C. Ramón Álvarez, V. Rodríguez Bouza, A. Soto Rodríguez, A. Trapote, C. Vico Villalba, P. Vischia

Instituto de Física de Cantabria (IFCA), CSIC-Universidad de Cantabria, Santander, Spain
S. Bhowmik, S. Blanco Fernández, I.J. Cabrillo, A. Calderon, J. Duarte Campderros, M. Fernandez, G. Gomez, C. Lasaosa García, R. Lopez Ruiz, C. Martinez Rivero, P. Martinez Ruiz del Arbol, F. Matorras, P. Matorras Cuevas, E. Navarrete Ramos, J. Piedra Gomez, L. Scodellaro, I. Vila, J.M. Vizan Garcia

University of Colombo, Colombo, Sri Lanka
B. Kailasapathy[58], D.D.C. Wickramarathna

University of Ruhuna, Department of Physics, Matara, Sri Lanka
W.G.D. Dharmaratna[59], K. Liyanage, N. Perera

CERN, European Organization for Nuclear Research, Geneva, Switzerland
D. Abbaneo, C. Amendola, E. Auffray, G. Auzinger, J. Baechler, D. Barney, A. Bermúdez Martínez, M. Bianco, A.A. Bin Anuar, A. Bocci, L. Borgonovi, C. Botta, E. Brondolin, C.E. Brown, C. Caillol, G. Cerminara, N. Chernyavskaya, D. d'Enterria, A. Dabrowski, A. David, A. De Roeck, M.M. Defranchis, M. Deile, M. Dobson, G. Franzoni, W. Funk, S. Giani, D. Gigi, K. Gill, F. Glege, J. Hegeman, J.K. Heikkilä, B. Huber, V. Innocente, T. James, P. Janot, O. Kaluzinska, O. Karacheban[27], S. Laurila, P. Lecoq, E. Leutgeb, C. Lourenço, L. Malgeri, M. Mannelli, M. Matthewman, A. Mehta, F. Meijers, S. Mersi, E. Meschi, V. Milosevic, F. Monti, F. Moortgat, M. Mulders, I. Neutelings, S. Orfanelli, F. Pantaleo, G. Petrucciani, A. Pfeiffer, M. Pierini, H. Qu, D. Rabady, B. Ribeiro Lopes, F. Riti, M. Rovere, H. Sakulin, R. Salvatico, S. Sanchez Cruz, S. Scarfi, C. Schwick, M. Selvaggi, A. Sharma, K. Shchelina, P. Silva, P. Sphicas[60], A.G. Stahl Leiton, A. Steen, S. Summers, D. Treille, P. Tropea, D. Walter, J. Wanczyk[61], J. Wang, S. Wuchterl, P. Zehetner, P. Zejdl, W.D. Zeuner

PSI Center for Neutron and Muon Sciences, Villigen, Switzerland
T. Bevilacqua[62], L. Caminada[62], A. Ebrahimi, W. Erdmann, R. Horisberger, Q. Ingram, H.C. Kaestli, D. Kotlinski, C. Lange, M. Missiroli[62], L. Noehte[62], T. Rohe, A. Samalan

ETH Zurich - Institute for Particle Physics and Astrophysics (IPA), Zurich, Switzerland
T.K. Aarrestad, M. Backhaus, G. Bonomelli, A. Calandri, C. Cazzaniga, K. Datta, P. De Bryas Dexmiers D'archiac[61], A. De Cosa, G. Dissertori, M. Dittmar, M. Donegà, F. Eble, M. Galli, K. Gedia, F. Glessgen, C. Grab, N. Härringer, T.G. Harte, D. Hits, W. Lustermann, A.-M. Lyon, R.A. Manzoni, M. Marchegiani, L. Marchese, A. Mascellani[61], F. Nessi-Tedaldi, F. Pauss, V. Perovic, S. Pigazzini, B. Ristic, R. Seidita, J. Steggemann[61], A. Tarabini, D. Valsecchi, R. Wallny

Universität Zürich, Zurich, Switzerland
C. Amsler[63], P. Bärtschi, M.F. Canelli, K. Cormier, M. Huwiler, W. Jin, A. Jofrehei, B. Kilminster, S. Leontsinis, S.P. Liechti, A. Macchiolo, P. Meiring, F. Meng, J. Motta, A. Reimers, P. Robmann, M. Senger, E. Shokr, F. Stäger, R. Tramontano

National Central University, Chung-Li, Taiwan
C. Adloff[64], D. Bhowmik, C.M. Kuo, W. Lin, P.K. Rout, P.C. Tiwari[37]

National Taiwan University (NTU), Taipei, Taiwan
L. Ceard, K.F. Chen, Z.g. Chen, A. De Iorio, W.-S. Hou, T.h. Hsu, Y.w. Kao, S. Karmakar, G. Kole, Y.y. Li, R.-S. Lu, E. Paganis, X.f. Su, J. Thomas-Wilsker, L.s. Tsai, D. Tsionou, H.y. Wu, E. Yazgan

High Energy Physics Research Unit, Department of Physics, Faculty of Science, Chulalongkorn University, Bangkok, Thailand
C. Asawatangtrakuldee, N. Srimanobhas, V. Wachirapusitanand

Tunis El Manar University, Tunis, Tunisia
Y. Maghrbi

Çukurova University, Physics Department, Science and Art Faculty, Adana, Turkey
D. Agyel, F. Boran, F. Dolek, I. Dumanoglu[65], E. Eskut, Y. Guler[66], E. Gurpinar Guler[66], C. Isik, O. Kara, A. Kayis Topaksu, Y. Komurcu, G. Onengut, K. Ozdemir[67], A. Polatoz, B. Tali[68], U.G. Tok, E. Uslan, I.S. Zorbakir

Middle East Technical University, Physics Department, Ankara, Turkey
G. Sokmen, M. Yalvac[69]

Bogazici University, Istanbul, Turkey
B. Akgun, I.O. Atakisi, E. Gülmez, M. Kaya[70], O. Kaya[71], S. Tekten[72]

Istanbul Technical University, Istanbul, Turkey
A. Cakir, K. Cankocak[65,73], G.G. Dincer[65], S. Sen[74]

Istanbul University, Istanbul, Turkey
O. Aydilek[75], B. Hacisahinoglu, I. Hos[76], B. Kaynak, S. Ozkorucuklu, O. Potok, H. Sert, C. Simsek, C. Zorbilmez

Yildiz Technical University, Istanbul, Turkey
S. Cerci, B. Isildak[77], D. Sunar Cerci, T. Yetkin

Institute for Scintillation Materials of National Academy of Science of Ukraine, Kharkiv,

Ukraine
A. Boyaryntsev, B. Grynyov

National Science Centre, Kharkiv Institute of Physics and Technology, Kharkiv, Ukraine
L. Levchuk

University of Bristol, Bristol, United Kingdom
D. Anthony, J.J. Brooke, A. Bundock, F. Bury, E. Clement, D. Cussans, H. Flacher, M. Glowacki, J. Goldstein, H.F. Heath, M.-L. Holmberg, L. Kreczko, S. Paramesvaran, L. Robertshaw, V.J. Smith, K. Walkingshaw Pass

Rutherford Appleton Laboratory, Didcot, United Kingdom
A.H. Ball, K.W. Bell, A. Belyaev[78], C. Brew, R.M. Brown, D.J.A. Cockerill, C. Cooke, A. Elliot, K.V. Ellis, K. Harder, S. Harper, J. Linacre, K. Manolopoulos, D.M. Newbold, E. Olaiya, D. Petyt, T. Reis, A.R. Sahasransu, G. Salvi, T. Schuh, C.H. Shepherd-Themistocleous, I.R. Tomalin, K.C. Whalen, T. Williams

Imperial College, London, United Kingdom
I. Andreou, R. Bainbridge, P. Bloch, O. Buchmuller, C.A. Carrillo Montoya, G.S. Chahal[79], D. Colling, J.S. Dancu, I. Das, P. Dauncey, G. Davies, M. Della Negra, S. Fayer, G. Fedi, G. Hall, A. Howard, G. Iles, C.R. Knight, P. Krueper, J. Langford, K.H. Law, J. León Holgado, L. Lyons, A.-M. Magnan, B. Maier, S. Mallios, M. Mieskolainen, J. Nash[80], M. Pesaresi, P.B. Pradeep, B.C. Radburn-Smith, A. Richards, A. Rose, K. Savva, C. Seez, R. Shukla, A. Tapper, K. Uchida, G.P. Uttley, T. Virdee[29], M. Vojinovic, N. Wardle, D. Winterbottom

Brunel University, Uxbridge, United Kingdom
J.E. Cole, A. Khan, P. Kyberd, I.D. Reid

Baylor University, Waco, Texas, USA
S. Abdullin, A. Brinkerhoff, E. Collins, M.R. Darwish, J. Dittmann, K. Hatakeyama, V. Hegde, J. Hiltbrand, B. McMaster, J. Samudio, S. Sawant, C. Sutantawibul, J. Wilson

Catholic University of America, Washington, DC, USA
R. Bartek, A. Dominguez, A.E. Simsek, S.S. Yu

The University of Alabama, Tuscaloosa, Alabama, USA
B. Bam, A. Buchot Perraguin, R. Chudasama, S.I. Cooper, C. Crovella, S.V. Gleyzer, E. Pearson, C.U. Perez, P. Rumerio[81], E. Usai, R. Yi

Boston University, Boston, Massachusetts, USA
A. Akpinar, C. Cosby, G. De Castro, Z. Demiragli, C. Erice, C. Fangmeier, C. Fernandez Madrazo, E. Fontanesi, D. Gastler, F. Golf, S. Jeon, J. O'cain, I. Reed, J. Rohlf, K. Salyer, D. Sperka, D. Spitzbart, I. Suarez, A. Tsatsos, A.G. Zecchinelli

Brown University, Providence, Rhode Island, USA
G. Barone, G. Benelli, D. Cutts, L. Gouskos, M. Hadley, U. Heintz, K.W. Ho, J.M. Hogan[82], T. Kwon, G. Landsberg, K.T. Lau, J. Luo, S. Mondal, T. Russell, S. Sagir[83], X. Shen, F. Simpson, M. Stamenkovic, N. Venkatasubramanian

University of California, Davis, Davis, California, USA
S. Abbott, B. Barton, C. Brainerd, R. Breedon, H. Cai,

M. Calderon De La Barca Sanchez, M. Chertok, M. Citron, J. Conway, P.T. Cox, R. Erbacher, F. Jensen, O. Kukral, G. Mocellin, M. Mulhearn, S. Ostrom, W. Wei, S. Yoo, F. Zhang

University of California, Los Angeles, California, USA
K. Adamidis, M. Bachtis, D. Campos, R. Cousins, A. Datta, G. Flores Avila, J. Hauser, M. Ignatenko, M.A. Iqbal, T. Lam, Y.f. Lo, E. Manca, A. Nunez Del Prado, D. Saltzberg, V. Valuev

University of California, Riverside, Riverside, California, USA
R. Clare, J.W. Gary, G. Hanson

University of California, San Diego, La Jolla, California, USA
A. Aportela, A. Arora, J.G. Branson, S. Cittolin, S. Cooperstein, D. Diaz, J. Duarte, L. Giannini, Y. Gu, J. Guiang, R. Kansal, V. Krutelyov, R. Lee, J. Letts, M. Masciovecchio, F. Mokhtar, S. Mukherjee, M. Pieri, D. Primosch, M. Quinnan, V. Sharma, M. Tadel, E. Vourliotis, F. Würthwein, Y. Xiang, A. Yagil

University of California, Santa Barbara - Department of Physics, Santa Barbara, California, USA
A. Barzdukas, L. Brennan, C. Campagnari, K. Downham, C. Grieco, M.M. Hussain, J. Incandela, J. Kim, A.J. Li, P. Masterson, H. Mei, J. Richman, S.N. Santpur, U. Sarica, R. Schmitz, F. Setti, J. Sheplock, D. Stuart, T.Á. Vámi, X. Yan, D. Zhang

California Institute of Technology, Pasadena, California, USA
S. Bhattacharya, A. Bornheim, O. Cerri, A. Latorre, J. Mao, H.B. Newman, G. Reales Gutiérrez, M. Spiropulu, J.R. Vlimant, C. Wang, S. Xie, R.Y. Zhu

Carnegie Mellon University, Pittsburgh, Pennsylvania, USA
J. Alison, S. An, P. Bryant, M. Cremonesi, V. Dutta, T. Ferguson, T.A. Gómez Espinosa, A. Harilal, A. Kallil Tharayil, C. Liu, T. Mudholkar, S. Murthy, P. Palit, K. Park, M. Paulini, A. Roberts, A. Sanchez, W. Terrill

University of Colorado Boulder, Boulder, Colorado, USA
J.P. Cumalat, W.T. Ford, A. Hart, A. Hassani, G. Karathanasis, N. Manganelli, J. Pearkes, C. Savard, N. Schonbeck, K. Stenson, K.A. Ulmer, S.R. Wagner, N. Zipper, D. Zuolo

Cornell University, Ithaca, New York, USA
J. Alexander, S. Bright-Thonney, X. Chen, D.J. Cranshaw, J. Dickinson, J. Fan, X. Fan, S. Hogan, P. Kotamnives, J. Monroy, M. Oshiro, J.R. Patterson, M. Reid, A. Ryd, J. Thom, P. Wittich, R. Zou

Fermi National Accelerator Laboratory, Batavia, Illinois, USA
M. Albrow, M. Alyari, O. Amram, G. Apollinari, A. Apresyan, L.A.T. Bauerdick, D. Berry, J. Berryhill, P.C. Bhat, K. Burkett, J.N. Butler, A. Canepa, G.B. Cerati, H.W.K. Cheung, F. Chlebana, G. Cummings, I. Dutta, V.D. Elvira, Y. Feng, J. Freeman, A. Gandrakota, Z. Gecse, L. Gray, D. Green, A. Grummer, S. Grünendahl, D. Guerrero, O. Gutsche, R.M. Harris, T.C. Herwig, J. Hirschauer, B. Jayatilaka, S. Jindariani, M. Johnson, U. Joshi, T. Klijnsma, B. Klima, K.H.M. Kwok, S. Lammel, C. Lee, D. Lincoln, R. Lipton, T. Liu, C. Madrid, K. Maeshima, C. Mantilla, D. Mason, P. McBride, P. Merkel,

S. Mrenna, S. Nahn, J. Ngadiuba, D. Noonan, S. Norberg, V. Papadimitriou, N. Pastika, K. Pedro, C. Pena[84], F. Ravera, A. Reinsvold Hall[85], L. Ristori, M. Safdari, E. Sexton-Kennedy, N. Smith, A. Soha, L. Spiegel, S. Stoynev, J. Strait, L. Taylor, S. Tkaczyk, N.V. Tran, L. Uplegger, E.W. Vaandering, I. Zoi

University of Florida, Gainesville, Florida, USA
C. Aruta, P. Avery, D. Bourilkov, P. Chang, V. Cherepanov, R.D. Field, C. Huh, E. Koenig, M. Kolosova, J. Konigsberg, A. Korytov, K. Matchev, N. Menendez, G. Mitselmakher, K. Mohrman, A. Muthirakalayil Madhu, N. Rawal, S. Rosenzweig, Y. Takahashi, J. Wang

Florida State University, Tallahassee, Florida, USA
T. Adams, A. Al Kadhim, A. Askew, S. Bower, R. Hashmi, R.S. Kim, S. Kim, T. Kolberg, G. Martinez, H. Prosper, P.R. Prova, M. Wulansatiti, R. Yohay, J. Zhang

Florida Institute of Technology, Melbourne, Florida, USA
B. Alsufyani, S. Butalla, S. Das, T. Elkafrawy[18], M. Hohlmann, E. Yanes

University of Illinois Chicago, Chicago, Illinois, USA
M.R. Adams, A. Baty, C. Bennett, R. Cavanaugh, R. Escobar Franco, O. Evdokimov, C.E. Gerber, M. Hawksworth, A. Hingrajiya, D.J. Hofman, J.h. Lee, D. S. Lemos, A.H. Merrit, C. Mills, S. Nanda, G. Oh, B. Ozek, D. Pilipovic, R. Pradhan, E. Prifti, T. Roy, S. Rudrabhatla, N. Singh, M.B. Tonjes, N. Varelas, M.A. Wadud, Z. Ye, J. Yoo

The University of Iowa, Iowa City, Iowa, USA
M. Alhusseini, D. Blend, K. Dilsiz[86], L. Emediato, G. Karaman, O.K. Köseyan, J.-P. Merlo, A. Mestvirishvili[87], O. Neogi, H. Ogul[88], Y. Onel, A. Penzo, C. Snyder, E. Tiras[89]

Johns Hopkins University, Baltimore, Maryland, USA
B. Blumenfeld, L. Corcodilos, J. Davis, A.V. Gritsan, L. Kang, S. Kyriacou, P. Maksimovic, M. Roguljic, J. Roskes, S. Sekhar, M. Swartz

The University of Kansas, Lawrence, Kansas, USA
A. Abreu, L.F. Alcerro Alcerro, J. Anguiano, S. Arteaga Escatel, P. Baringer, A. Bean, Z. Flowers, D. Grove, J. King, G. Krintiras, M. Lazarovits, C. Le Mahieu, J. Marquez, M. Murray, M. Nickel, M. Pitt, S. Popescu[90], C. Rogan, C. Royon, S. Sanders, C. Smith, G. Wilson

Kansas State University, Manhattan, Kansas, USA
B. Allmond, R. Gujju Gurunadha, A. Ivanov, K. Kaadze, Y. Maravin, J. Natoli, D. Roy, G. Sorrentino

University of Maryland, College Park, Maryland, USA
A. Baden, A. Belloni, J. Bistany-riebman, Y.M. Chen, S.C. Eno, N.J. Hadley, S. Jabeen, R.G. Kellogg, T. Koeth, B. Kronheim, Y. Lai, S. Lascio, A.C. Mignerey, S. Nabili, C. Palmer, C. Papageorgakis, M.M. Paranjpe, E. Popova[91], A. Shevelev, L. Wang

Massachusetts Institute of Technology, Cambridge, Massachusetts, USA
J. Bendavid, I.A. Cali, P.c. Chou, M. D'Alfonso, J. Eysermans, C. Freer, G. Gomez-Ceballos, M. Goncharov, G. Grosso, P. Harris, D. Hoang, D. Kovalskyi, J. Krupa, L. Lavezzo, Y.-J. Lee, K. Long, C. Mcginn, A. Novak, M.I. Park,

C. Paus, C. Reissel, C. Roland, G. Roland, S. Rothman, G.S.F. Stephans, Z. Wang, B. Wyslouch, T. J. Yang

University of Minnesota, Minneapolis, Minnesota, USA
B. Crossman, B.M. Joshi, C. Kapsiak, M. Krohn, D. Mahon, J. Mans, B. Marzocchi, M. Revering, R. Rusack, R. Saradhy, N. Strobbe

University of Nebraska-Lincoln, Lincoln, Nebraska, USA
K. Bloom, D.R. Claes, G. Haza, J. Hossain, C. Joo, I. Kravchenko, A. Rohilla, J.E. Siado, W. Tabb, A. Vagnerini, A. Wightman, F. Yan, D. Yu

State University of New York at Buffalo, Buffalo, New York, USA
H. Bandyopadhyay, L. Hay, H.w. Hsia, I. Iashvili, A. Kalogeropoulos, A. Kharchilava, M. Morris, D. Nguyen, S. Rappoccio, H. Rejeb Sfar, A. Williams, P. Young

Northeastern University, Boston, Massachusetts, USA
G. Alverson, E. Barberis, J. Bonilla, B. Bylsma, M. Campana, J. Dervan, Y. Haddad, Y. Han, I. Israr, A. Krishna, J. Li, M. Lu, R. Mccarthy, D.M. Morse, V. Nguyen, T. Orimoto, A. Parker, L. Skinnari, E. Tsai, D. Wood

Northwestern University, Evanston, Illinois, USA
J. Bueghly, S. Dittmer, K.A. Hahn, D. Li, Y. Liu, M. Mcginnis, Y. Miao, D.G. Monk, M.H. Schmitt, A. Taliercio, M. Velasco

University of Notre Dame, Notre Dame, Indiana, USA
G. Agarwal, R. Band, R. Bucci, S. Castells, A. Das, R. Goldouzian, M. Hildreth, K. Hurtado Anampa, T. Ivanov, C. Jessop, K. Lannon, J. Lawrence, N. Loukas, L. Lutton, J. Mariano, N. Marinelli, I. Mcalister, T. McCauley, C. Mcgrady, C. Moore, Y. Musienko[22], H. Nelson, M. Osherson, A. Piccinelli, R. Ruchti, A. Townsend, Y. Wan, M. Wayne, H. Yockey, M. Zarucki, L. Zygala

The Ohio State University, Columbus, Ohio, USA
A. Basnet, M. Carrigan, L.S. Durkin, C. Hill, M. Joyce, M. Nunez Ornelas, K. Wei, D.A. Wenzl, B.L. Winer, B. R. Yates

Princeton University, Princeton, New Jersey, USA
H. Bouchamaoui, K. Coldham, P. Das, G. Dezoort, P. Elmer, A. Frankenthal, B. Greenberg, N. Haubrich, K. Kennedy, G. Kopp, S. Kwan, D. Lange, A. Loeliger, D. Marlow, I. Ojalvo, J. Olsen, D. Stickland, C. Tully, L.H. Vage

University of Puerto Rico, Mayaguez, Puerto Rico, USA
S. Malik, R. Sharma

Purdue University, West Lafayette, Indiana, USA
A.S. Bakshi, S. Chandra, R. Chawla, A. Gu, L. Gutay, M. Jones, A.W. Jung, A.M. Koshy, M. Liu, G. Negro, N. Neumeister, G. Paspalaki, S. Piperov, V. Scheurer, J.F. Schulte, M. Stojanovic, J. Thieman, A. K. Virdi, F. Wang, A. Wildridge, W. Xie, Y. Yao

Purdue University Northwest, Hammond, Indiana, USA
J. Dolen, N. Parashar, A. Pathak

Rice University, Houston, Texas, USA
D. Acosta, A. Agrawal, T. Carnahan, K.M. Ecklund, P.J. Fernández Manteca,

S. Freed, P. Gardner, F.J.M. Geurts, I. Krommydas, W. Li, J. Lin, O. Miguel Colin, B.P. Padley, R. Redjimi, J. Rotter, E. Yigitbasi, Y. Zhang

University of Rochester, Rochester, New York, USA
A. Bodek, P. de Barbaro, R. Demina, J.L. Dulemba, A. Garcia-Bellido, O. Hindrichs, A. Khukhunaishvili, N. Parmar, P. Parygin[91], R. Taus

Rutgers, The State University of New Jersey, Piscataway, New Jersey, USA
B. Chiarito, J.P. Chou, S.V. Clark, D. Gadkari, Y. Gershtein, E. Halkiadakis, M. Heindl, C. Houghton, D. Jaroslawski, S. Konstantinou, I. Laflotte, A. Lath, R. Montalvo, K. Nash, J. Reichert, P. Saha, S. Salur, S. Schnetzer, S. Somalwar, R. Stone, S.A. Thayil, S. Thomas, J. Vora, H. Wang

University of Tennessee, Knoxville, Tennessee, USA
D. Ally, A.G. Delannoy, S. Fiorendi, S. Higginbotham, T. Holmes, A.R. Kanuganti, N. Karunarathna, L. Lee, E. Nibigira, S. Spanier

Texas A&M University, College Station, Texas, USA
D. Aebi, M. Ahmad, T. Akhter, K. Androsov[61], O. Bouhali[92], R. Eusebi, J. Gilmore, T. Huang, T. Kamon[93], H. Kim, S. Luo, R. Mueller, D. Overton, D. Rathjens, A. Safonov

Texas Tech University, Lubbock, Texas, USA
N. Akchurin, J. Damgov, N. Gogate, A. Hussain, Y. Kazhykarim, K. Lamichhane, S.W. Lee, A. Mankel, T. Peltola, I. Volobouev

Vanderbilt University, Nashville, Tennessee, USA
E. Appelt, Y. Chen, S. Greene, A. Gurrola, W. Johns, R. Kunnawalkam Elayavalli, A. Melo, F. Romeo, P. Sheldon, S. Tuo, J. Velkovska, J. Viinikainen

University of Virginia, Charlottesville, Virginia, USA
B. Cardwell, H. Chung, B. Cox, J. Hakala, R. Hirosky, A. Ledovskoy, C. Neu

Wayne State University, Detroit, Michigan, USA
S. Bhattacharya, P.E. Karchin

University of Wisconsin - Madison, Madison, Wisconsin, USA
A. Aravind, S. Banerjee, K. Black, T. Bose, E. Chavez, S. Dasu, P. Everaerts, C. Galloni, H. He, M. Herndon, A. Herve, C.K. Koraka, A. Lanaro, R. Loveless, J. Madhusudanan Sreekala, A. Mallampalli, A. Mohammadi, S. Mondal, G. Parida, L. Pétré, D. Pinna, A. Savin, V. Shang, V. Sharma, W.H. Smith, D. Teague, H.F. Tsoi, W. Vetens, A. Warden

Authors affiliated with an international laboratory covered by a cooperation agreement with CERN
S. Afanasiev, V. Alexakhin, D. Budkouski, I. Golutvin†, I. Gorbunov, V. Karjavine, V. Korenkov, A. Lanev, A. Malakhov, V. Matveev[94], V. Palichik, V. Perelygin, M. Savina, V. Shalaev, S. Shmatov, S. Shulha, V. Smirnov, O. Teryaev, N. Voytishin, B.S. Yuldashev[95], A. Zarubin, I. Zhizhin, Yu. Andreev, A. Dermenev, S. Gninenko, N. Golubev, A. Karneyeu, D. Kirpichnikov, M. Kirsanov, N. Krasnikov, I. Tlisova, A. Toropin

Authors affiliated with an institute formerly covered by a cooperation agreement with CERN
G. Gavrilov, V. Golovtcov, Y. Ivanov, V. Kim[96], P. Levchenko[97], V. Murzin, V. Oreshkin, D. Sosnov, V. Sulimov, L. Uvarov, A. Vorobyev†, T. Aushev,

K. Ivanov, V. Gavrilov, N. Lychkovskaya, A. Nikitenko[98,99], V. Popov, A. Zhokin, M. Chadeeva[96], R. Chistov[96], S. Polikarpov[96], V. Andreev, M. Azarkin, M. Kirakosyan, A. Terkulov, E. Boos, V. Bunichev, M. Dubinin[84], L. Dudko, A. Ershov, V. Klyukhin, O. Kodolova[99], S. Obraztsov, M. Perfilov, S. Petrushanko, V. Savrin, G. Vorotnikov, V. Blinov[96], T. Dimova[96], A. Kozyrev[96], O. Radchenko[96], Y. Skovpen[96], V. Kachanov, S. Slabospitskii, A. Uzunian, A. Babaev, V. Borshch, D. Druzhkin

†: Deceased
[1]Also at Yerevan State University, Yerevan, Armenia
[2]Also at TU Wien, Vienna, Austria
[3]Also at Ghent University, Ghent, Belgium
[4]Also at Universidade do Estado do Rio de Janeiro, Rio de Janeiro, Brazil
[5]Also at FACAMP - Faculdades de Campinas, Sao Paulo, Brazil
[6]Also at Universidade Estadual de Campinas, Campinas, Brazil
[7]Also at Federal University of Rio Grande do Sul, Porto Alegre, Brazil
[8]Also at University of Chinese Academy of Sciences, Beijing, China
[9]Also at China Center of Advanced Science and Technology, Beijing, China
[10]Also at University of Chinese Academy of Sciences, Beijing, China
[11]Also at China Spallation Neutron Source, Guangdong, China
[12]Now at Henan Normal University, Xinxiang, China
[13]Also at University of Shanghai for Science and Technology, Shanghai, China
[14]Now at The University of Iowa, Iowa City, Iowa, USA
[15]Also at an institute formerly covered by a cooperation agreement with CERN
[16]Also at Zewail City of Science and Technology, Zewail, Egypt
[17]Also at British University in Egypt, Cairo, Egypt
[18]Now at Ain Shams University, Cairo, Egypt
[19]Also at Purdue University, West Lafayette, Indiana, USA
[20]Also at Université de Haute Alsace, Mulhouse, France
[21]Also at Istinye University, Istanbul, Turkey
[22]Also at an international laboratory covered by a cooperation agreement with CERN
[23]Also at The University of the State of Amazonas, Manaus, Brazil
[24]Also at University of Hamburg, Hamburg, Germany
[25]Also at RWTH Aachen University, III. Physikalisches Institut A, Aachen, Germany
[26]Also at Bergische University Wuppertal (BUW), Wuppertal, Germany
[27]Also at Brandenburg University of Technology, Cottbus, Germany
[28]Also at Forschungszentrum Jülich, Juelich, Germany
[29]Also at CERN, European Organization for Nuclear Research, Geneva, Switzerland
[30]Also at HUN-REN ATOMKI - Institute of Nuclear Research, Debrecen, Hungary
[31]Now at Universitatea Babes-Bolyai - Facultatea de Fizica, Cluj-Napoca, Romania
[32]Also at MTA-ELTE Lendület CMS Particle and Nuclear Physics Group, Eötvös Loránd University, Budapest, Hungary
[33]Also at HUN-REN Wigner Research Centre for Physics, Budapest, Hungary
[34]Also at Physics Department, Faculty of Science, Assiut University, Assiut, Egypt
[35]Also at Punjab Agricultural University, Ludhiana, India
[36]Also at University of Visva-Bharati, Santiniketan, India
[37]Also at Indian Institute of Science (IISc), Bangalore, India
[38]Also at Amity University Uttar Pradesh, Noida, India
[39]Also at IIT Bhubaneswar, Bhubaneswar, India
[40]Also at Institute of Physics, Bhubaneswar, India

[41]Also at University of Hyderabad, Hyderabad, India
[42]Also at Deutsches Elektronen-Synchrotron, Hamburg, Germany
[43]Also at Isfahan University of Technology, Isfahan, Iran
[44]Also at Sharif University of Technology, Tehran, Iran
[45]Also at Department of Physics, University of Science and Technology of Mazandaran, Behshahr, Iran
[46]Also at Department of Physics, Faculty of Science, Arak University, ARAK, Iran
[47]Also at Helwan University, Cairo, Egypt
[48]Also at Italian National Agency for New Technologies, Energy and Sustainable Economic Development, Bologna, Italy
[49]Also at Centro Siciliano di Fisica Nucleare e di Struttura Della Materia, Catania, Italy
[50]Also at Università degli Studi Guglielmo Marconi, Roma, Italy
[51]Also at Scuola Superiore Meridionale, Università di Napoli 'Federico II', Napoli, Italy
[52]Also at Fermi National Accelerator Laboratory, Batavia, Illinois, USA
[53]Also at Lulea University of Technology, Lulea, Sweden
[54]Also at Consiglio Nazionale delle Ricerche - Istituto Officina dei Materiali, Perugia, Italy
[55]Also at Institut de Physique des 2 Infinis de Lyon (IP2I), Villeurbanne, France
[56]Also at Department of Applied Physics, Faculty of Science and Technology, Universiti Kebangsaan Malaysia, Bangi, Malaysia
[57]Also at Consejo Nacional de Ciencia y Tecnología, Mexico City, Mexico
[58]Also at Trincomalee Campus, Eastern University, Sri Lanka, Nilaveli, Sri Lanka
[59]Also at Saegis Campus, Nugegoda, Sri Lanka
[60]Also at National and Kapodistrian University of Athens, Athens, Greece
[61]Also at Ecole Polytechnique Fédérale Lausanne, Lausanne, Switzerland
[62]Also at Universität Zürich, Zurich, Switzerland
[63]Also at Stefan Meyer Institute for Subatomic Physics, Vienna, Austria
[64]Also at Laboratoire d'Annecy-le-Vieux de Physique des Particules, IN2P3-CNRS, Annecy-le-Vieux, France
[65]Also at Near East University, Research Center of Experimental Health Science, Mersin, Turkey
[66]Also at Konya Technical University, Konya, Turkey
[67]Also at Izmir Bakircay University, Izmir, Turkey
[68]Also at Adiyaman University, Adiyaman, Turkey
[69]Also at Bozok Universitetesi Rektörlügü, Yozgat, Turkey
[70]Also at Marmara University, Istanbul, Turkey
[71]Also at Milli Savunma University, Istanbul, Turkey
[72]Also at Kafkas University, Kars, Turkey
[73]Now at Istanbul Okan University, Istanbul, Turkey
[74]Also at Hacettepe University, Ankara, Turkey
[75]Also at Erzincan Binali Yildirim University, Erzincan, Turkey
[76]Also at Istanbul University - Cerrahpasa, Faculty of Engineering, Istanbul, Turkey
[77]Also at Yildiz Technical University, Istanbul, Turkey
[78]Also at School of Physics and Astronomy, University of Southampton, Southampton, United Kingdom
[79]Also at IPPP Durham University, Durham, United Kingdom
[80]Also at Monash University, Faculty of Science, Clayton, Australia
[81]Also at Università di Torino, Torino, Italy
[82]Also at Bethel University, St. Paul, Minnesota, USA
[83]Also at Karamanoğlu Mehmetbey University, Karaman, Turkey

[84]Also at California Institute of Technology, Pasadena, California, USA
[85]Also at United States Naval Academy, Annapolis, Maryland, USA
[86]Also at Bingol University, Bingol, Turkey
[87]Also at Georgian Technical University, Tbilisi, Georgia
[88]Also at Sinop University, Sinop, Turkey
[89]Also at Erciyes University, Kayseri, Turkey
[90]Also at Horia Hulubei National Institute of Physics and Nuclear Engineering (IFIN-HH), Bucharest, Romania
[91]Now at another institute formerly covered by a cooperation agreement with CERN
[92]Also at Texas A&M University at Qatar, Doha, Qatar
[93]Also at Kyungpook National University, Daegu, Korea
[94]Also at another international laboratory covered by a cooperation agreement with CERN
[95]Also at Institute of Nuclear Physics of the Uzbekistan Academy of Sciences, Tashkent, Uzbekistan
[96]Also at another institute formerly covered by a cooperation agreement with CERN
[97]Also at Northeastern University, Boston, Massachusetts, USA
[98]Also at Imperial College, London, United Kingdom
[99]Now at Yerevan Physics Institute, Yerevan, Armenia